Carbon Capture Science & Technology 13 (2024) 100293

Contents lists available at ScienceDirect

Carbon Capture Science & Technology

journal homepage: www.elsevier.com/locate/ccst

Review

CO_2 capture via subsurface mineralization geological settings and engineering perspectives towards long-term storage and decarbonization in the Middle East

Priyanka Kumari[a,b,c], Rihab Yahmadi[a], Fatima Mumtaz[a,b], Lourdes F. Vega[a,b,c], Andrea Ceriani[c,d], Riccardo Tribuzio[e,f,g], Ludovic F. Dumée[a,b,c,*], Alessandro Decarlis[c,d,**]

[a] Department of Chemical and Petrochemical Engineering, Khalifa University, PO Box 127788, Abu Dhabi, United Arab Emirates
[b] Research and Innovation Center on 2D Nanomaterials (RIC2D), Khalifa University, PO Box 127788, Abu Dhabi, United Arab Emirates
[c] Research and Innovation Center on CO_2 and Hydrogen (RICH Center), Khalifa University, PO Box 127788, Abu Dhabi, United Arab Emirates
[d] Department of Earth Sciences, Khalifa University, PO Box 127788, Abu Dhabi, United Arab Emirates
[e] Dipartimento di Scienze della Terra e dell'Ambiente, Universita' di Pavia, Pavia, Italy
[f] Istituto Geoscienze e Georisorse, Consiglio Nazionale delle Ricerche, Pavia, Italy
[g] Istituto Nazionale di Oceanografia e di Geofisica Sperimentale, Sgonico, Trieste, Italy

A R T I C L E I N F O

Keywords:
Mineral carbonation
Geological sequestration
CO_2 capture scale-up
Techno-economic analysis

A B S T R A C T

Mineral carbonation or mineralization of CO_2 using rocks or waste industrial materials is emerging as a viable carbon capture and storage (CCS) technology, especially for smaller and medium-scale emitters where geological sequestration is not feasible. During mineralization processes, CO_2 chemically reacts with alkaline earth metals in waste materials or rocks to form stable and non-toxic carbonates *In situ* mineral carbonation holds promise due to ample resources and enhanced security. However, it is still in its early stages, with higher transport and storage costs compared to geological storage in sedimentary basins. *Ex situ* mineral carbonation has shown promise at pilot and demonstration scales, but its widespread application is hindered by high costs, ranging from US$50-US$300/ton of sequestered CO_2. This review delves into the current progress of proposed mineralization technologies and their potential in reducing the overall cost of CO_2 sequestration. The discussion critically analyzes various factors affecting carbonation reactions, such as temperature, pressure, leaching agents, solid-to-liquid ratio, and mineralogy for geological settings relevant to the Middle East and the net-zero strategy established within Gulf Cooperation Countries (GCC). Furthermore, the potential commercialization of mineral carbonation, emphasizing the importance of reducing energy consumption and production costs to make the process economically viable is highlighted, offering directions for circular economy and mineral carbonation as a substantial carbon mitigation tool in the Middle East region. Life Cycle Assessment and Techno-Economic Analysis) was also reviewed to provide a comprehensive understanding of both the environmental and economic implications of a CO_2 capture via subsurface mineralization

1. Introduction

The Arabian Peninsula and countries within the Gulf Cooperation Council (GCC) rely extensively on fossil fuel sources to reach their energy targets, and greenhouse gas emissions (GHG) have therefore been in constant growth across the entire region since the early 1990's (Jamil et al., 2016). To avoid further global warming and reduce the impact of climate change, the Intergovernmental Panel on Climate Change (IPCC) stressed the critical need to prevent CO_2 emissions to the atmosphere (IPCC, 2018), and over 10 Gton of CO_2 shall be avoided by 2050 to maintain the warming trend below the threshold of 1.5 to 2 °C increase compared to 1990's average temperatures (Dumée et al., 2012;

Abbreviations: CCUS, Carbon Capture, Utilization, and Storage; GCC, Gulf Cooperation Council; GHG, Greenhouse gas emissions; S/L, Solid to liquid; LNG, Liquified natural gas; LCA, Life Cycle Assessment; ÅAU, Åbo Akademi University; GWP, Global Warming Potential; NETL, National Energy Technology Laboratory; NGCC, Natural gas combined cycle; RCA, Recycled concrete aggregate; CSTR, Continuous Stirred Tank Reactor; RPB, Rotary packed bed; MSWI, Municipal solid waste incineration ash.

* Corresponding author.
** Corresponding author at: Research and Innovation Center on CO_2 and Hydrogen (RICH Center), Khalifa University, PO Box 127788, Abu Dhabi, United Arab Emirates.
E-mail addresses: Ludovic.dumee@ku.ac.ae (L.F. Dumée), Alessandro.decarlis@ku.ac.ae (A. Decarlis).

https://doi.org/10.1016/j.ccst.2024.100293
Received 16 June 2024; Received in revised form 26 August 2024; Accepted 4 September 2024

Maina et al., 2021). Such policies are reflected in major initiatives, such as the target of net zero emissions by 2050 pledged by the United Arab Emirates (UAE Net Zero 2050) (Lahn, 2021), multiple other countries worldwide. In addition, the energy roadmaps developed by most GCC countries, and focused on blue or green hydrogen production and export to third party countries, will further increase carbon emissions and requires immediate action to limit the footprint and future commercial developments (Lahn, 2021).

A diverse array of innovative techniques designed to mitigate greenhouse gas emissions are currently in practice. Chemical absorption, for instance, involves the use of solvents or absorbents to capture CO_2 from industrial flue gases. However, this method often requires significant energy input for solvent regeneration and can result in the release of harmful chemicals (Babamohammadi et al., 2015). Adsorption techniques utilize porous materials such as activated carbon or metal-organic frameworks to trap CO_2 molecules, yet they face limitations in terms of capacity, selectivity, and regeneration efficiency (Zhou et al., 2019). Membrane separation methods selectively permeate CO_2 through membranes, but challenges include membrane fouling, high capital costs, and limited scalability (Shah et al., 2020). Biological processes, such as algae-based capture or enhanced photosynthesis in plants, offer the potential for sustainable CO_2 removal, but they require extensive land or water resources and face scalability issues (Paul et al., 2021). Despite their promise, these CCS methods are still in various stages of development and face significant technological, economic, and environmental challenges that must be addressed for widespread implementation.

Carbon Capture, Utilization, and Storage (CCUS) strategies are designed to mitigate greenhouse gas emissions, particularly CO_2, by capturing it from industrial processes or directly from the atmosphere and supporting either direct industrial utilization or underground storage to prevent its release into the atmosphere (Kelemen et al., 2020). Mineral carbonation processes, whereby CO_2 is reacted with transition metals present within waste materials or rocks, to generate carbonates minerals, appear to offer a positive compromise to respect environmental policies and ensure stable and effective carbon fixation. The resulting carbonate products are thermally and chemically stable as well as non-toxic, but usually form aggregates composed of different carbonate minerals depending on the source of reactants that can be used for various civil engineering applications. Mineral carbon capture, also known as mineral carbonation or mineralization, is a process that involves capturing carbon dioxide (CO_2) from the atmosphere or industrial sources and converting it into stable mineral forms. The carbonation strategies can be categorized as either *ex-situ* or *in-situ. Ex-situ* mineral carbonization involves the extraction of minerals from their natural deposits and bringing them to the surface for carbonation reactions. Once the minerals are extracted, they are crushed or ground into fine particles to increase their surface area and enhance reactivity (Gerdemann et al., 2004) . The *ex-situ* mineral storage options were examined by the US Department of Energy, involving investigations into kinetics, process development, and economic assessments (Gerdemann et al., 2004). Their findings indicated that approximately 55,000 ton of mineral feedstock would be necessary to carbonate the daily CO_2 emissions from a 1 GW coal-fired power plant, rendering it an impractical solution for such significant sources. Despite this, many have regarded it as a viable option for smaller industrial carbon sources (Gerdemann et al., 2004). *In-situ* mineral carbonation involve carbonation reactions taking place underground, within the natural geological formations where CO_2 is injected into subsurface formations containing suitable reactive minerals, such as ultramafic rocks or basalts (Gerdemann et al., 2004). The *in-situ* mineral carbonation of the peridotites in Oman has been estimated to have consumed over 1 $GtCO_2$ via *in-situ* carbonation (Kelemen et al., 2020). Thus, the scope of *in-situ* mineral carbonation is broader compared to *ex-situ* methods (Kelemen et al., 2020).

Properties of the reacting rocks, such as the specific surface area available for the reactions or minerals content and solubility, will greatly vary based on the geological setting, and lead to various fractured structures with specific pores connectivity as well as overall porosity (Romano et al., 2013). The Arabian plate is largely composed of volcanic and igneous rocks with high reaction potential which offers great potential for carbon mineral storage, which may lead to direct underground capture or reaction with mined minerals (Hunt et al., 2010). Various carbonation strategies, previously discussed at large (Koytsoumpa et al., 2018), have been proposed to mitigate or prevent CO_2 emissions, including improved long-term storage and smart utilization of CO_2 generated during industrial processes or power generation, with published reviews covering different aspects of it. For instance, a review on the geochemical aspects of CO_2 sequestration in deep saline aquifers evaluated the impact of factors on the solubility trapping effectiveness, with a mix of both experimental and modelling investigations (De Silva et al., 2015). *In-situ* mineralization of CO_2 in basalt rocks and challenges related to the technical and operational challenges (Raza et al., 2022) was also assessed, while recent advances to enable CO_2 fixation through mineralization for carbon capture and storage (CCS) was also discussed at high level (Snæbjörnsdóttir et al., 2020). Advances related to CO_2 storage and the preservation of caprock integrity, with a focus on prominent operational sequestration initiatives, geological sequestration methodologies, and the dynamics of CO_2 migration within reservoir rock formations were equally addressed (Shukla et al., 2010). Links between the geological settings and availability of local rocks with the reactivity and storage of the minerals at relevant capture scales are however yet to be fully determined.

This article tackles this gap by presenting a cross-over analysis between geological and reaction engineering approaches to enable mineral carbon fixation, relevant to the Arabian Peninsula. The perspective is focused on the reactivity of the rocks and minerals present across the region and discusses previous scale-up attempts at global level to propose a roadmap for long-term and effective carbon mineral storage in the region. A critical discussion is focused around three major pillars including the availability of minerals, their accessibility and reactivity and a technical-economic analysis towards decarbonization and large-scale capture strategies. This critical analysis offers a perspective towards emerging challenges and benefits of large-scale implementation of CCUS in the region. A circular economy approach is required to ensure that the potential of the GCC region to mitigate carbon emissions produced locally is fully exploited, and to utilize local resources as carbon sinks to manage supplementary emissions generated by the emerging Hydrogen economy, will be discussed.

2. Geological setting and resources within the Arabian plate

In this section, the geological setting of the Arabian plate will be discussed to showcase the types and availability of both minerals and rocks, relevant to carbon capture. The Arabian plate offers promising mineral resources for carbon mineralization in terms of composition, volume, and strategic location (Vahrenkamp et al., 2021). Two main associations of igneous rocks can be regarded as excellent candidates for permanent mineral carbon storage. These sites are located (i) along the North-Eastern boundary of the plate, along the Bitlis-Zagros suture Zone and in the Hajar Mountains, primarily in the territories of Oman and UAE, and (ii) close to the western boundary in the volcanic fields of Saudi Arabia and Yemen (Fig. 1(a)).

2.1. Geological resources in North-eastern boundary

Several mafic and ultramafic rocks are exposed along and close to the Bitlis-Zagros suture zone, mostly deriving from the closure of the Tethys Ocean during the late Mesozoic. These rocks are ophiolites, which represent slabs of fossil oceanic lithosphere that were accreted during the continental collision between the Arabian and the Eurasian plates. The nature of the rocks varies and mainly comprises mantle peridotites, gabbros and basalts, with variable degree of deformation and alteration (Moghadam and Stern, 2015). Peridotite is found in ophiolites, which

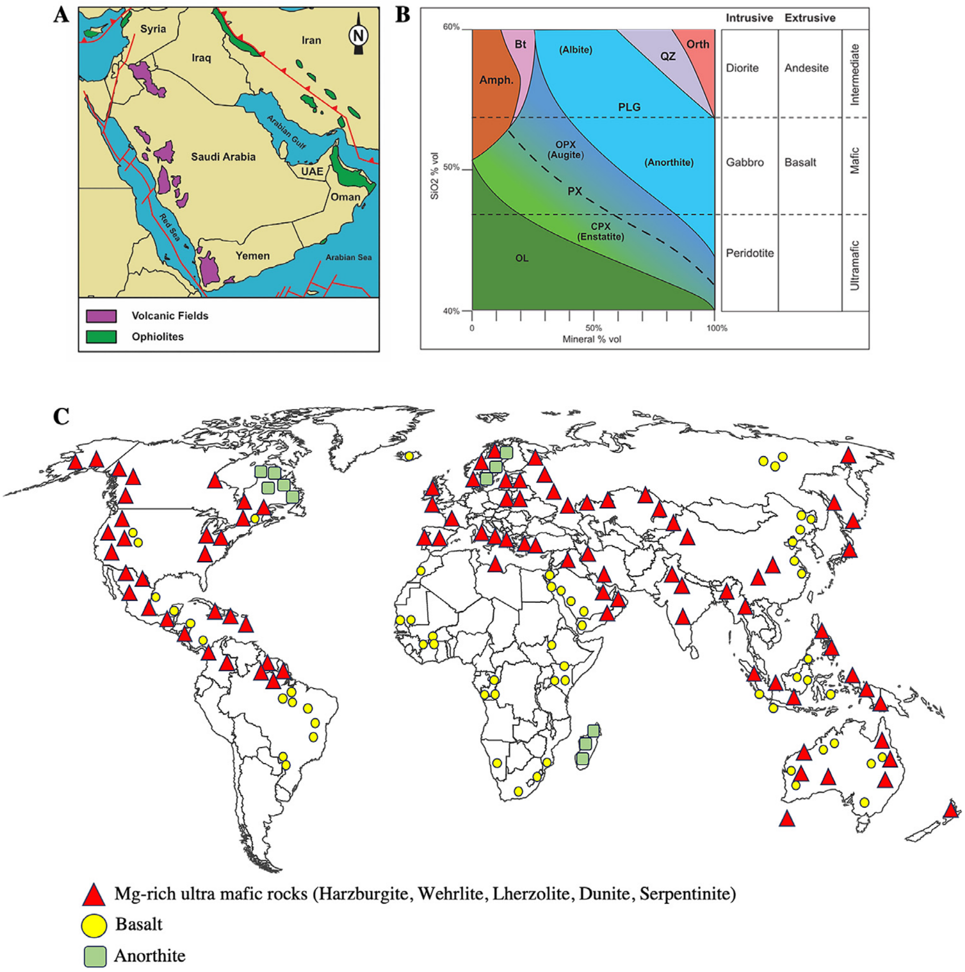

Fig. 1. (A) Geological schematic of possible geological resources for carbonation via natural rocks mineralization in the Arabian Peninsula; (B) Proportional mineral composition of igneous rocks (Clark, 1966); (C) Major Mg-rich ultramafic, basalt and anorthite rock feedstock regions in the world, adapted from (Sanna et al., 2014).

are intricate geological formations that represent the uplift of segments of oceanic crust onto land. The largest such outcrop globally is the Samail Ophiolite in Oman, spanning approximately 350 km in length, 40 km in width, and an average thickness of 5 km, with around 30 % of its volume consisting of mantle peridotite (Sanna et al., 2014).

The Southernmost rock bodies, which are represented by the Hajar Mountains of Oman and UAE, consist of a nappe stack including several tectonic units of continental and oceanic affinity. Geophysical and structural field studies in the UAE-Oman mountain belt reveal that the ca.10–15 km sequence of Semail ophiolite was emplaced from NE to SW onto the Arabian continental margin during the Late Cretaceous initially along a NE-dipping subduction zone (Searle et al., 2022; Searle and Ali, 2009; Searle and Cox, 2002; Searle et al., 2015), which evolved into a thin-skin fold and thrust belt with time. The orogen formed because of the closure of the Paleotethys Ocean that bounded the UAE to the North and East since the Paleozoic. The subsequent oblique collision of the Arabian passive margin with Eurasian plate, a polyphase process initiated at the end of the Mesozoic, led to the formation of the Zagros mountains in the north. The system was complicated by a peculiar structural setting, which includes a prominent right-lateral strike slip fault (Minab fault) separating the Zagros suture zones from a subduction zone (Makran). Close to this junction, south-east of the Zagros mountains, since late Cretaceous large portions of the former oceanic crust escaped subduction, were eradicated, and translated onto the Arabian continental margin units, thereby forming the Hajar Mountains. Today, the Oceanic sequence occupies the highest structural position in the Hajar orogen in a nappe stack composed of different superimposed tectonic units. They form an East-dipping pile that crops out from UAE to the Oman (N-S), and they extend offshore under the recent marine sediments for tens of kilometers (Ali et al., 2020). The UAE-Oman oceanic rocks belong the well-known Semail supergroup. Semail ophiolite is a lithostratigraphic unit formed by a Cretaceous oceanic basement and the related sedimentary cover (Dilek, 2003). After the Penrose conference (1972) and for a long time, it was regarded as the archetype of the oceanic crust (Peltonen, 2005). Fig. 1(b) shows the relationships among different igneous rocks forming the classic Penrose-type ophiolite, a model-based, layer-cake stratigraphic succession that starts with an ultramafic complex, composed of mantle peridotite variably altered to serpentinite. The ultramafic complex is covered by a gabbroic complex, which typically includes minor cumulus peridotites and pyroxenites, in turn covered by the sheeted dyke complex, which consists of subparallel subvolcanic intrusions. A volcanic complex, usually formed by extrusive products as pillow basalts, and submarine sedimentary rocks are also present.

2.2. Geological resources in western boundary

The western side of the region is dominated by basement rocks and associated rifted basins facing the Red Sea margin. Since the Oligocene to modern times, the area was interested by an extensive volcanism that generated the so-called “Harrats”, large volcanic fields where basalts spread at the surface generating effusive expanses of lavas and cones. Lavas generally followed rifting-related fractures (Moufti et al., 2012) to form one of the most extensive alkali-basaltic-to-tholeiitic provinces in the world (Chorowicz, 2005; Moucha and Forte, 2011). The thickness of felsic volcanics is on average of ~100 m or below, but may locally reach a few hundred meters in thickness (Vahrenkamp et al., 2021). Harrats volcanism has been associated to partial melting of a mantle source retaining a moderate proportion of crustal component (Downs et al., 2019).

Effusive products generated by multiple eruptions led to the accumulation of overlapping basaltic lava flows that spread out from Yemen to the Northern Saudi Arabia coastal premises. Evidence for recent volcanism has been also reported in the Red Sea offshore, both on the Saudi margin (Cochran, 2005) and on the Egyptian margin (Ali et al., 2020), although a direct correlation with the harrats system has not been fully demonstrated. Volcanic activity seems to rejuvenate from Yemen, where they date 30–20 Ma (Moufti et al., 2013) towards the north, where, for instance, Harrat Ithnayn records ages up to 500–120 Ka (Alhejji et al., 2019). This trend and the progressive increase of volcanic activity in the last 10 Ma, was interpreted as a northward progradation of the Afar mantle plume (Camp and Roobol, 1992).

These volcanic rocks offer a high level of intrinsic porosity as well as typically high calcium or magnesium contents, making them promising for *in situ* carbonation reactions. The following section will present the reactivity of locally assessed rocks or similar rocks to evaluate the potential towards carbon capture and most beneficial economic models to support carbon management at the region level.

3. Carbon mineralization process and lab-scale testing

A comprehensive analysis of the reaction kinetics pertaining to an array of minerals and rocks that hold significance within the context of the Arabian Peninsula is presented in this section. The discussion is primarily centered around gaining a deeper understanding of these kinetics, their implications, and relevance to the region's geological and environmental considerations.

3.1. Mineral carbon capture process

Mafic and ultramafic rocks are geological formations abundant in silicate minerals. These rocks serve as potential candidates for carbon sequestration through a process known as silicate mineral carbonation. The fundamentals of silicate carbonation involve the chemical reaction between CO_2 and the silicate minerals present in these rocks, which are found to follow an Urey type reaction (Daval et al., 2009; Urey and Korff, 1952). In this process, CO_2 from the atmosphere dissolves in water, forming carbonic acid (H_2CO_3), which reacts with silicate minerals to produce carbonate minerals (such as calcite or magnesite) and dissolved ions. Here, CO_2 reacts with water and calcium silicate to form calcium carbonate (a stable carbonate mineral) and silicic acid. In the context of carbon sequestration, this reaction is accelerated under controlled conditions of temperature, pressure, and pH to enhance the rate of carbonation (Teir et al., 2007b). By promoting this reaction, CO_2 is effectively trapped in the form of stable carbonate minerals, thus mitigating its release into the atmosphere. Each phase occurs across specific temperature, pressure, pH ranges and are affected by the contact area with the rocks. This contact area depends on the porosity-permeability of the rock bodies, which in case of igneous rocks, is mostly dependent on fractures and intrinsic porosity of the material.

Amongst all relevant rocks available for carbon mineral storage, only pillow basalts, produced during submarine volcanic eruptions and whereby magma outpours overlap sequentially with rapid cooling steps supporting entrapment of gas bubbles, leaving spaces between the lava flows, own a significant primary porosity, which is implicitly linked to their emplacement mechanisms (Snæbjörnsdóttir et al., 2020). The pillow basalts with altered, fractured zones exhibit the highest porosity, reaching up to 20 %. Hydrothermal fluids circulate through the bedrock, with the overlying deposits providing effective sealing that allows prolonged water-rock interactions and facilitates chemical reactions with the surrounding altered basalt. The CO_2 injection target involves a volume of 7800 km^3 of altered basalt with an average porosity of 10 % in the region of Juan de Fuca Plate, offshore western USA, offering a storage potential of 920 Gt of CO_2 (Sanna et al., 2014). Intracrystalline cavities in gabbro and peridotites are limited, and porosity is mainly related to fractures generated at different stages during obduction of the nappes.

3.2. Minerals reactivity

Data on the rates of carbonation potential and kinetics of primary minerals composing mafic and ultramafic rocks obtained during lab-scale testing by different authors are presented and discussed here. Olivine, serpentine, wollastonite, pyroxene, brucite, and magnetite are frequently assessed for carbonation reactions due to their chemical characteristics and prevalence in mafic and ultramafic rock formations (O'Connor et al., 2002). Olivine, abundant in Earth's mantle and certain igneous rocks, reacts rapidly with CO_2 to generate carbonate minerals like magnesite, making it appealing for its rapid kinetics and potential for substantial carbon sequestration (O'Connor et al., 2002). Serpentine minerals, found in hydrated magnesium silicates commonly present in ultramafic rocks, undergo carbonation to produce stable carbonate minerals such as magnesite, facilitated by their fibrous structure which enhances reaction surface area (Park and Fan, 2004). Wollastonite, a calcium silicate mineral, exhibits rapid carbonation potential due to its high calcium content (Huijgen, W.J.J. et al., 2007). Pyroxene minerals contribute to carbon storage by forming carbonate minerals like calcite or magnesite (Schott et al., 1981). Brucite, a magnesium hydroxide mineral, reacts vigorously with CO_2, offering promise for carbon sequestration (Zhao et al., 2010). These minerals are attractive for carbonation due to their CO_2 reactivity, abundance in relevant rock types, and potential for significant carbon capture. Olivine, Serpentine, Wollastonite, Pyroxene, Brucite and Magnetite were tested in different experimental conditions, whereby the impact of temperature, partial pressure of CO2 (PCO_2), solution chemistry and particle size on the carbonation reaction rate are evaluated. These minerals are rich in MgO and CaO, which are most essential for the formation of carbonates at ambient conditions with high reactivity. Unless otherwise stated, kinetic experiments reported were conducted in continuously stirred autoclave reactors and for each test, a fixed amount of mineral reactant was mixed with a carrier solution, usually distilled water, or bicarbonate/salt solution, pressurized within a range between 20 and 150 bar at 70 to 200 °C and for durations between 1 and 20 h (Gerdemann, S. J. et al., 2007; Haug et al., 2010; Kwak et al., 2011; Summers et al., 2005).

Eq. (1) (Penner et al., 2004b) was used to calculate the reaction rates and assess the impact of operational factors, such as pH, temperature, ions concentration, as well as catalytic or inhibitory chemicals concentrations on the reaction rate.

$$\text{Reaction rate (\%) (r)} = \frac{\text{change in carbonation potential (\%)}}{\text{change in time}} \tag{1}$$

The carbonation potential, shown in Eq. (2) (Penner et al., 2004b), was used to express the CO_2 sequestration reaction efficiency (Rx), which corresponds to the percentage stoichiometric conversion of reactive ions, such as Mg^{2+}, $Ca^{2+}$and Fe^{2+}cations in silicate feed to carbonate.

$$Rx = \frac{\text{xCO2}}{\varepsilon A(1 - xCO2)} \tag{2}$$

where xCO_2 corresponds to the weight percent of CO_2 contained within the solid products and εA to the percent weight added if all the available cations convert to carbonates (Penner et al., 2004a). The liquid to solid ratio (L/S) was often used to reflect on the ratio of solution to solid rock used and is expressed in g g^{-1}. In addition, unless otherwise specified, analytical grade and dry CO_2 gas were used within the experiments.

3.2.1. Olivine

Olivine is a nesosilicate formed by a solid solution between the end members Forsterite (Mg-rich) and Fayalite (Fe-rich). Olivine forms up to 90% vol of mafic rocks and more than 90 % vol of ultramafic rocks.

Table 1
Carbonation experiments for minerals performed under different reaction conditions; deionised water (DI), Not Available (NA); unless otherwise specified, the main solvent is reported as water.

Entry	Mineral	CO_2 Pressure (bar)	Temperature (°C)	Particle Size (μm)	Solution	Time (h)	R_x (%)	Ref.
1	Olivine	115	185	NA	DI	0.16	27	(Haug et al., 2010)
2	Olivine	115	185	NA	DI	1	32	(Haug et al., 2010)
3	Olivine	150	185	38	0.64 M $NaHCO_3$, 1 M NaCl	1	39.6	(Gerdemann, Stephen J. et al., 2007)
4	Olivine	60	185	38	0.64 M $NaHCO_3$, 1 M NaCl	1	25.7	(Gerdemann, Stephen J. et al., 2007)
5	Olivine	150	185	75	0.64 M $NaHCO_3$ 1 M NaCl	1	5.1	(Summers et al., 2005)
6	Olivine	97	80	NA	DI	20	8	(Kwak et al., 2011)
7	Lizardite	150	185	38	0.64 M $NaHCO_3$ 1 M NaCl	1	2.5	(Gerdemann, Stephen J. et al., 2007)
8	Lizardite	150	185	37	0.64 M $NaHCO_3$, 1 M NaCl	1	40	(O'Connor et al., 2002)
9	Serpentine	126	155	37	0.64 M NaHCO3 1 M NaCl	1	60	(Maroto-Valer et al., 2005a)
10	Serpentine	1	70	75	1 vol% orthophosphoric acid, 0.9 wt% of oxalic acid and 0.1 wt% EDTA	1	65	(Park and Fan, 2004)
11	Serpentine	1	30	NA	4 M HCl, HNO_3, H_2SO_4, NaOH	0.5	94	(Teir et al., 2007b)
12	Serpentine	1	90	NA	1.4 M NH_4HSO_4, NH_4HCO_3 and NH_3	0.5	95.5	(Wang and Maroto-Valer, 2011)
13	Serpentine	40	30–100	NA	HCl/NH_3	1	73.6	(Zhang et al., 2012)
14	Serpentine	40	180	NA	HCl/NH_3	1	55.8	(Zhang et al., 2012)
15	Wollastonite	20	200	37	DI	0.25	70	(Huijgen and Comans, 2006)
16	Wallastonite	30	80		Succinic or Acetic acid	1	90	(Bałdyga et al., 2010)
17	Wallastonite	40	100	38	DI	1	80	(O'Connor et al., 2002)
18	Wallastonite	20	200	38	DI	0.25	75	(Huijgen, Wouter J. J. et al., 2006a)
19	Pyroxene	150	185	37	0.64 M NaOH, 1 M NaCl	1	33	(O'Connor et al., 2002)
20	Brucite	15	25	<150	DI	0.5	3.4	(Zhao et al., 2010)
21	Brucite	15	25	<150	DI	2.5	98	(Zhao et al., 2010)
22	Brucite	15	25	<150	0.39 M HCl	0.5	5.6	(Zhao et al., 2010)
23	Brucite	15	25	<150	0.39 M HCl	2.5	58.6	(Zhao et al., 2010)
24	Magnetite	150	185	37	1 M NaCl 0.64 M $NaHCO_3$	1	8	(O'Connor et al., 2005)

Forsterite is a very reactive mineral, which constitutes the most abundant phase in the Harzburgite (mantle peridotite) of the UAE (Eq. (3)).

$$Mg_2SiO_4 + 4H^+ \rightarrow 2Mg^{2+} + 2H_2O + SiO_2 \tag{3}$$

Olivine is reported as one of the most Mg rich reactive minerals to date and extensively evaluated for CO_2 mineral storage by carbonation. Olivine carbonation proceeded to 27 % in 10 min **(**Table 1**, Entry 1)** and 32 % in 1 h at 185 °C and 115 bar in an aqueous deionised solution **(**Table 1**, Entry 2)** leading to a kinetics constant of 0.03 h^{-1} (Haug et al., 2010). The rate of carbonation reaction can be increased by the use of inorganic salts as additives such as $NaHCO_3$, $KHCO_3$ and NaCl (Giammar et al., 2005). Experiments conducted in 1 M NaCl and 0.64 M $NaHCO_3$ at 185 °C temperature and 150 bar pressure with 38 μm particle size and achieved 39.6 % conversion within 1 h **(**Table 1**, Entry 3)** (Gerdemann, Stephen J. et al., 2007). In addition, tests performed with the same experimental conditions but at a lower operating pressure of 60 bar led to decrease in the carbonation potential to 25.7 % from 39.6 % **(**Table 1**, Entry 4)** (Gerdemann, Stephen J. et al., 2007). As the particle size increased from 38 to 75 μm, the carbonation potential increase by 8 times **(**Table 1**, Entry 5)** (Summers et al., 2005). Direct carbonation at 80 °C, using deionised water with a L/S of 1 at 97 bar, achieved a conversion of 8 % after 20 h **(**Table 1**, Entry 6)** (Kwak et al., 2011).

3.2.2. *Serpentine*

Serpentine is a group of phyllosilicates (Lizardite, Antigorite and Chrysotile polymorphs) which forms in natural environments when olivine in ultramafic and mafic rocks reacts with water and CO_2 at temperature <500 °C (Eq. (4)).

$$4Mg_2SiO_4(Forsterite) + 4H_2O + 2CO_2 = 2Mg_3Si_5O_5(OH)_4(\text{Serpentine}) + 2MgCO_3\ (\text{Magnesite}) \tag{4}$$

This reaction has important implications for the alteration of ultramafic rocks, but it is also fundamental to understand important crustal-scale processes at oceanic and proto-oceanic domains. Serpentine may also derive from the breakdown of calcium-rich pyroxene with H_2.

$$3CaMgSi_2O_6(Diopside) + 6\text{H}^+ \rightarrow Mg_3Si_2O_5(OH)_4(Serpentine)\ 3\text{Ca}^{2+} + H_2O\ +\ 4\ SiO_2\ (\text{Quartz}) \tag{5}$$

The conversion of Serpentine, sourced from Cedar Hills (Pennsylvania, USA) to Magnesite was performed under various conditions. At 155 °C and 126 bar for particles of either 37 of 75 μm in size and tested over 1 h using a 1 M NaCl and 0.6 M $NAHCO_3$ solution and a L/S of 12, the conversion reached 60 % **(**Table 1**, Entry 9)** (Maroto-Valer et al., 2005a). The conversion increased to 65 % when performed at 70 °C and 1 bar for ~75 μm particle size for 1 h using a solution composed of 1 vol% orthophosphoric acid, 0.9 wt% of oxalic acid and 0.1 wt% EDTA at a L/S of 15 mg/mL **(**Table 1**, Entry 10)** (Park and Fan, 2004). Several acids and bases such as HCl, HNO_3, H_2SO_4, NaOH were also trialled to increase the dissolution kinetics of Serpentine and subsequently the carbonation efficiency (Maroto-Valer et al., 2005b; Sanna et al., 2014; Teir et al., 2007b). The carbonation efficiency of Serpentine achieved ~94 % at 30 °C and 1 bar using solutions containing HCl, HNO_3, H_2SO_4, NaOH for 0.5 h **(**Table 1**, Entry 11)** (Teir et al., 2007b) and 95.5 % at 90 °C and 1 bar using solutions containing NH_4HSO_4, NH_4HCO_3 and NH_3 within 0.5 h **(**Table 1**, Entry 12)** (Wang and Maroto-Valer, 2011). The carbonation reaction of Serpentine was also carried out in a stirred autoclave with a volume of 1 L at 40 bar for 1 h using HCl/NH_3 as a solution and a L/S ratio of 2. The carbonation efficiency increases to a maximum of 73.6 % as the temperature increases from 30 °C to 100 °C, and it decreases to 55.8 % at 180 °C **(**Table 1**, Entries 13 and 14)** (Zhang et al., 2012).

Carbonation with Lizardite in 1 M NaCl and 0.64 M $NaHCO_3$ at 185 °C temperature and 150 bar pressure with 38 μm particle size and achieved 2.5 % conversion in 1 h **(**Table 1**, Entry 7)**. The reaction rate for Lizardite was found to be 16 times lower than Olivine under the same carbonation conditions (Gerdemann, Stephen J. et al., 2007). The reaction efficiency of Lizardite containing 20.7 wt% of Mg, 0.3 wt% of Ca and 1.5 wt% Fe, reached 40 % in a solution composed of 0.64 M NaOH and 1 M NaCl at 185 °C and 150 bar with 37 μm particle size in 1 h **(**Table 1**, Entry 8)** (O'Connor et al., 2002).

3.2.3. Wollastonite

The dissolution mechanism as for the case of wollastonite ($CaSiO_3$) is represented in Eq. (6) (Huijgen, Wouter J. J. et al., 2006b), which leads to the saturation of Ca^{+2} ions in the solution, which further reaction with bicarbonate ions to form carbonates .

$$CaSiO_3\ (\text{Wollastonite}\ ) + 2H^+ \rightarrow Ca^{2+} + H_2O + SiO_2 \tag{6}$$

Wollastonite was reported as one of the most Ca rich reactive minerals, reaching over 70 % carbonation potential in 0.25 h at 200 °C and 20 bar for particles of 38 μm in size through direct aqueous carbonation (Huijgen and Comans, 2006) **(**Table 1**, Entry 15)**. Another experiment conducted with Wollastonite reached 90 % at 80 °C and 30 bar for 1 h using either pure succinic or acetic acid solution at a L/S of 1 **(**Table 1**, Entry 16)** (Bałdyga et al., 2010). The reaction efficiency of Wollastonite corresponding to the stoichiometric conversion of Ca^{2+}, Fe^{2+} and Mg^{2+} in a silicate feed to carbonate reached 80 % at 100 °C and 40 bar within 1 h **(**Table 1**, Entry 17)** (O'Connor et al., 2002) and 75 % at 200 °C and 20 bar in 0.25 h, for a L/S of 5 **(**Table 1**, Entry 18)** (Huijgen, Wouter J. J. et al., 2006a).

3.2.4. Pyroxene

Pyroxene is a group of inosilicates typically found in mafic and ultramafic rocks. Several studies (McAdam et al., 2008), showed that Augite has a higher dissolution rate than diopside independently from the pH of the solution. Low temperature experiments using acid solutions (pH 1–6) showed a linear kinetics for the dissolution of selected pyroxenes (Enstatite, Diopside) with preferential release of Ca and Mg (Schott et al., 1981). Thus, Ca (Diopside, Eq. (6); Augite, Eq. (7)) and high-Fe pyroxenes (Hedembergite, Eq. (8)) may significantly contribute to the divalent cations budget during dissolution. (Eq. (8)).

$$MgCaSi_2O_6 + 4H^+ \rightarrow Mg^{2+} + Ca^{2+} + 2H_2O + 2SiO_2 \tag{7}$$

$$\begin{aligned}(Ca, Mg, Fe^{2+}, Fe^{3+},\ Ti,\ Al)_2\ (Si,\ Al)_2O_6 + 4H^+ \rightarrow Fe^{2+}\\ + Ca^{2+} + 2H_2O + 2SiO_2\end{aligned} \tag{8}$$

$$FeCaSi_2O_6 + 4H^+ \rightarrow Fe^{2+} + Ca^{2+} + 2H_2O + 2SiO_2 \tag{9}$$

The reaction efficiency of Augite, composed at 6.9 wt% of Mg, 15.6 wt% of Ca and 9.6wt% of Fe reached 33 % in an aqueous solution composed of 0.64 M NaOH and 1 M NaCl at 185 °C and 150 bar with 37 μm particle size within 1 h **(**Table 1**, Entry 19)** (O'Connor et al., 2002).

3.2.5. Brucite

Various reaction routes can potentially result in the formation of Nesquehonite within aqueous settings where solid phase brucite ($Mg(OH)_2$) and gaseous phase CO_2 are present. One possible pathway involves a single-step heterogeneous reaction between hydrated CO_2 and brucite as shown in Eq. (10) (Zhao et al., 2010)."

$$Mg(OH)_2\ (\text{Brucite}\ ) + CO_2\ .\ H_2O \rightarrow MgCO_3.H_2O \tag{10}$$

The conversion of Brucite performed at room temperature and 15 bar and 0.5 h for particles of <150 µm size using a deionised water at a L/S ratio of 14, led to a conversion up to 3.4 % **(**Table 1**, Entry 20)**. The conversion increases to 98 % after 2.5 h **(**Table 1**, Entry 21)** corresponding to a kinetic constant of 48.54 h^{-1}. When performed in the same conditions but using a 0.39 M HCL solution, the carbonation efficiency increase up to 5.6 % for 0.5 h **(**Table 1**, Entry 22)** and 58.6 % after 2.5 h **(**Table 1**, Entry 23)** corresponding to a kinetic constant of 29.014 h^{-1}. Analysis of the solution chemistry shows that, as expected, the HCl slurry exhibits higher concentrations of Mg^{2+} compared to DI water throughout the experiments, indicating more extensive dissolution of brucite in the acidic environment. However, charge balance analysis reveals that the concentration of HCO^{3-} in HCl falls below that in DI water after about 2 h. Moreover, the lower pH of the HCl solution results in a reduction of ${CO_3}^{2-}$ concentration by roughly 50 %. Over time, the difference in Mg^{2+} concentration between the two solutions decreases from around 250 % at 15 min to approximately 17 % at 135 min (Zhao et al., 2010). These combined effects may have adversely affected the crystallization of carbonate phases, resulting in a lower extent of carbonation in the HCl solution. Therefore, the addition of acids or bases generally enhances the dissolution of minerals and accelerates reaction kinetics, but this effect is significant only if the reactions are conducted for short periods. If the reaction continues for longer durations (>2 h), the acidic solution may have the opposite effect on the reaction kinetics (Zhao et al., 2010).

3.2.6. Magnetite

Research demonstrated that iron oxides possess active surface sites capable of interacting with gaseous CO_2 molecules. Due to its thermodynamic properties, iron acts as a potent reducing agent, consequently Eq. (11) contains the proposed initial carbonation reactions (Mora Mendoza et al., 2019).

$$Fe_3O_4(\text{Magnetite}) + Fe + 4CO_2\ \rightarrow 4FeCO_3 \tag{11}$$

The reaction efficiency of Magnetite reached 8 % in an aqueous solution composed of 0.64 M $NaHCO_3$ and 1 M NaCl at 185 °C and 150 bar for a mean particle size of 37 μm, within 1 h **(**Table 1**, Entry 24)** (O'Connor et al., 2005).

3.3. Rocks reactivity

This section highlights the carbonation yield, and rates of kinetics of typical rocks that can be carbonated including Harzburgite, Wehrlite, Lherzolite, Dunite, Serpentinite, Basalt and Anorthosite from diverse locations (Fig. 1(c)) are presented. Harzburgite, Wehrlite, Lherzolite, Dunite, Serpentinite are rich in olivine, pyroxene and/or serpentine, which are essential minerals for the formation of carbonates with high reactivity. Basalt and Anorthosite also include a high proportion of plagioclase. The experiments were generally performed in lab-based conditions with 0.1 to 2 L stirred autoclave reactors at pressures ranging between 1 and 130 bar, temperatures of 23.5 to 185 °C and durations of 1 to 1460 h.

3.3.1. Harzburgite

Harzburgite was collected from New Caledonia (France), and contains 88 wt % Serpentine, 10 wt % Olivine and accessory Orthopyroxene, with a bulk chemistry characterized by 0.9 wt% CaO and 40.4 wt % MgO. The rock was tested in 2 L stirred autoclave reactors at 180 °C temperature and over a 10 to 20 bar pressure with < 100 μm particle

Table 2
Carbonation experiments for rocks performed under different carbonation reaction conditions; deionised water is referenced as DI; details on the seawater composition are not systematically provided; unless otherwise specified, the solution was aqueous.

Entry	Rock	CO_2 Pressure (bar)	Temperature (°C)	Time (h)	Particle Size (μm)	Solution	Rx (%)	Ref.
1	Harzburgite	10	180	24	<100	DI	4	(Bodénan et al., 2014)
2	Harzburgite	20	80	24	<100	DI	4.85	(Bodénan et al., 2014)
3	Harzburgite	1	23.5	1460	105	Seawater (pH 8.5, Conductivity 50,000 μS/cm)	7.6	(Rigopoulos et al., 2018)
4	Wehrlite	10	180	96	100	DI	0.49	(Bodénan et al., 2014)
5	Wehrlite	65± 5	185± 2 °C	2	21.9–26.2	0.64 M $NaHCO_3$ and 1 M NaCl	44.9	(Li et al., 2022)
6	Lherzolite	10	180	96	200	DI	1.05	(Bodénan et al., 2014)
7	Dunite	1	23.5	1460	150	Seawater	7.4	(Rigopoulos et al., 2018)
8	Dunite	130	180	0.8	2000–3000	0.64 M $NaHCO_3$	15	(Rashid et al., 2023)
9	Dunite	130	180	1.7	2000–3000	0.64 M $NaHCO_3$	20	(Rashid et al., 2023)
10	Dunite	130	180	3.3	2000–3000	0.64 M $NaHCO_3$	25	(Rashid et al., 2023)
11	Basalt	1	23.5	1460	104–150	Seawater (pH 8.1, Conductivity 65,000 μS/cm)	2.1	(Rigopoulos et al., 2018)
12	Basalt	150	185	1	37	1 M NaCl 0.64 $NaHCO_3$	15	(O'Connor et al., 2005)
13	Anorthosite	40	200	24	75–150	DI	4	(Munz et al., 2012)
14	Anorthosite	100	200	24	75–150	DI	7	(Munz et al., 2012)
15	Anorthosite	100	200	48	75–150	DI	11	(Munz et al., 2012)
16	Anorthosite	100	200	24	75–150	$CaCl_2$ (3.5 g/L)	15	(Munz et al., 2012)
17	Serpentinite	19–21	485	0.25	<74	5 M HCl	14	(Romão et al., 2016)
18	Serpentinite	19–21	510	0.5	<74	5 M HCl	70.3	(Romão et al., 2016)
19	Serpentinite	19–21	515	0.5	74–250	5 M HCl	38.8	(Romão et al., 2016)
20	Serpentinite	51–74	535	0.25	63–100	$(NH_4)_2SO_4$, NH_4OH (0.003 g/L)	65	(Stasiulaitiene et al., 2014)
21	Mine waste rock	60	185	0.5	106	1 M NaCl 0.64 M $NaHCO_3$	15	(Li and Hitch, 2017)
22	Mine waste rock	60	185	2	106	1 M NaCl 0.64 M $NaHCO_3$	31.7	(Li and Hitch, 2017)
23	Iron mine waste	1	80	1	<63	1 M NaCl 0.64 M $NaHCO_3$, pH 8	Fe= 5.32 Ca=5.23	(Kusin et al., 2023)
24	Iron mine waste	1	80	1	<63	1 M NaCl 0.64 M $NaHCO_3$, pH 8	Fe= 5.62 Ca=5.61	(Kusin et al., 2023)

over a period of 24 to 96 h using deionized water and 90 g/L as sample concentration. The carbonation potential, tested over 24 h, was found to be dependent on the reactor pressure, with a relative 1.5 times increase between 10 and 20 bar from 4 % (Table 2, **Entry 1)** to 4.85 % (Table 2, **Entry 2)**. The kinetics constant reached 0.073 h^{-1} at 10 bar and 0.11 h^{-1} at 20 bar (Bodénan et al., 2014).

Harzburgite collected from Troodos ophiolite complex (Cyprus), containing around 70 wt% Olivine, ~25 wt% Pyroxene and 2–3 wt% Serpentine, as well as accessory Talc and Chlorite (corresponding to bulk 0.51 wt% CaO and 21.9 wt% MgO), were trialled (Rigopoulos et al., 2018). The carbonation experiment was performed with a 1 L stirred autoclave reactors in ambient conditions, at 23.5 °C and 1 bar, with 105 μm particle size over 1460 h using a sea water solution, with an initial pH of 8.2 and 2 g/L as sample concentration. The carbonation potential increased by 13 times by increasing the specific surface area from 0.5 to 53.1 m^2g^{-1}, from 0.6 % for unmilled Harzburgite up to 7.6 % for the milled Harzburgite samples (Table 2**, Entry 3)** (Rigopoulos et al., 2018).

3.3.2. Wehrlite

Wehrlite was collected from New Caledonia, France, and mostly consists of Serpentine associated with 6 wt% Olivine and minor Clinopyroxene, with a bulk chemistry characterized by 4.9 wt% CaO and 32 wt% MgO. The wehrlite was trialled within 2 L stirred autoclave reactor at 180 °C and 10 bar pressure for particles around 100 μm for 96 h using deionized water with 90 g/L sample concentration (Table 2**, Entry 4)**. The carbonation potential reached 0.49 % for a kinetics constant of 0.005 h^{-1} (Bodénan et al., 2014).

Wehrlite was collected from the Turnagain ultramafic complex in British Columbia, Canada, and mostly consists of 59 wt% Olivine, 21 wt% Ca-Clinopyroxene, 14 wt% Lizardite, 3.9 wt% Magnetite and 0.4 wt% Brucite. The rocks were tested in a 0.1 L Hastelloy-C Parr bench-top stirred autoclave to determine the stoichiometric magnesium silicate to magnesium carbonate conversion extent achievable at 185 ± 2 °C and 65 ± 5 bar pressure. The experiment used 15 % solid reactant material in a fluid composition of 0.64 M $NaHCO_3$ and 1 M NaCl within the bench-top stirred reactor, with a constant stirrer speed of 1450 ± 50 rpm (Table 2**, Entry 5)** (Li et al., 2022). The sample was run for a 2 h testing period achieved 44.9 % a carbonation conversion, whereas a serpentinized wehrlite collected from same area and composed of 57 wt% Forsterite, 4.6 wt% Diopside, 31 wt% Lizardite, 5.3 wt% Magnetite and 2 wt% Brucite reached 26 % of carbonation conversion at same test conditions (Li et al., 2022).

3.3.3. Lherzolite

Lherzolite was collected from French Pyrenees (France), and is mainly composed of Serpentine, 6 wt% Olivine and minor Clinopyroxene and Orthopyroxene, with a bulk chemistry characterized by 5 wt% CaO and 31 wt % MgO. This rock was tested in 2 L stirred autoclave reactors at 180 °C and 10 bar for particles on the order of 200 μm with deionized water at a concentration of 90 g/L (Table 2**, Entry 6)** (Bodénan et al., 2014). A carbonation potential of 1.05 % was achieved within 96 h for a kinetics constant of 0.01 h^{-1} (Bodénan et al., 2014).

3.3.4. Dunite

The rock sourced from Troodos ophiolite complex (Cyprus) contains around 97 wt% Olivine and accessory Serpentine, Talc and Chlorite, and correspond to bulk CaO and MgO values of 0.33 wt% and 46.1 wt%, respectively. The carbonation potential of Dunite into Calcite was 0.7 % for unmilled Dunite and 7.4 % for milled Dunite tested within a 1 L stirred autoclave reactor at 23.5 °C and 1 bar with particles ranging from 104 to 150 μm in size, using sea water at pH 8.2 with 2 g/L sample concentration for 1460 h (Table 2**, Entry 7)** (Rigopoulos et al., 2018). The kinetics constant reached of 0.005 h^{-1} in these conditions but the conversion factor was not explicitly provided (Rigopoulos et al., 2018).

Dunite rocks containing 61–62 wt% Lizardite, 30–33 wt% Olivine, 3.8–8.3 wt% Brucite, 0.6 wt % Magnetite (corresponding to bulk 25.8 wt% MgO and 14.4 wt% SiO_2) were used for carbonation experiments performed in a 0.3 L high pressure reactor at 180 ˚C and 130 bar with 2–3 mm particles for 6 h using 0.64 M $NaHCO_3$ brines (Rashid et al., 2023). A carbonation potential of 15 % in 0.8 h (Table 2, **Entry 8)**, 20 % in 1.7 h (Table 2, **Entry 9)** and 25 % in 3.3 h (Table 2, **Entry 10)** was achieved leading to a kinetic constant of 0.002 h^{-1} (Rashid et al., 2023).

3.3.5. Basalt

Basalt samples were collected from Troodos ophiolite complex (Cyprus), containing >50 wt% calcic plagioclase, ~20 wt% Augitef followed by ~10 wt% olivine, ~5 wt% Chlorite and ~5 wt% opaque minerals. The basalts were tested in 1 L stirred autoclave reactors at 23.5 ˚C and 1 bar for mixed particles sizes ranging between 104 and 150 μm using sea water at a pH 8.2 with 2 g/L sample concentration for 1460 h (Table 2, **Entry 11)**. The carbonation potential reached 2.1 % with a kinetics constant of 0.0014 h^{-1} (Rigopoulos et al., 2018).

A basalt containing Olivine, Plagioclase, Augite and Magnetite as minerals were analysed, without providing the bulk chemical compositions. The rock was treated at 185 ˚C and 150 bar for 37 μm particles sizes using 1 M NaCl, 0.64 M $NaHCO_3$ with 15 % solids sample for 1 h (Table 2, **Entry 12)** reached 15 % carbonation conversion (O'Connor et al., 2005).

3.3.6. Anorthosite

Anorthosite from Sogn (Norway) composed of 92–95 wt % plagioclase and other minor minerals such as Amphibole, Biotite, Epidote, Chlorite and Scapolite (corresponding to bulk 0) was tested. The rock contains 0.13 wt% MgO and 14.0 wt% CaO, and was used in aqueous batch experiments at temperatures ranging between 100, 200 and 250 ˚C, pressures between 20, 40 and 100 bar with CO_2 as the pressurising medium and for particles size distributions ranging between 75 and 150 μm (Munz et al., 2012). The autoclaves were loaded with 5 g of starting material and either 40 mL of deionized water or 40 mL deionized water mixed added $CaCl_2$ at a concentration of 3.5 g/L. As the reactor pressure increased from 40 to 100 bar using deionised water, the carbonation potential increased from 4 to 7 % at 200 ˚C within a 24 h window (Table 2, **Entries 13 and 14)**. Increasing the reaction duration to 48 h, supported the carbonation potential with an increased to 11 % (Table 2, **Entry 15).** Additional tests using $CaCl_2$ in deionised water were performed at 200 ˚C and 100 bar for 24 h. The carbonation potential increased to 15 % (Table 2, **Entry 16)**, which was twice higher than that carried without the $CaCl_2$ in otherwise the same experimental conditions (Munz et al., 2012).

3.3.7. Serpentinite

Serpentinite mined from a quarry (Portugal) containing Serpentine and Olivine as well as a minor fraction (<10 wt%) of Talc and Tremolite, corresponding to 0.18 wt% CaO and 22.15 MgO bulk compositions, was used for carbonation reactions. The carbonation tests were performed at 21 bar and within a 485–515 ˚C in the stirred reactor using an aqueous solution of HCl. At 485 ˚C temperature condition, 21 bar pressure and particle size < 74 µm using HCl solution, the carbonation potential reached 14 % in 0.25 h (Table 2, **Entry 17)**, which further increased to 70.3 % as the temperature increased to 510 ˚C in 0.5 h (Table 2, **Entry 18)**. On increasing particle size from 75 µm up to 250 µm at 21 bar, the carbonation potential reduced to 38.8 % (Table 2, **Entry 19)** as the surface area reduced to half on increasing the particle size (Romão et al., 2016).

Serpentinite sourced from Lithuania containing Lizardite, Clinochrysotile and Antigorite, corresponding to a bulk composition characterized by 35.4 wt% MgO, 14.1 wt% Fe_2O_3 and 0.34 wt% CaO, was used for carbonation experiments performed in a heated vertical reactor at 535 ˚C and 51–74 bar with 63–100 µm particles using $(NH_4)_2SO_4$, NH_4OH (Table 2, **Entry 20)**. A carbonation potential of 65 % was achieved within 0.25 h (Stasiulaitiene et al., 2014).

3.3.8. Listwaenite

Listwaenite is a rock produced by the reaction of serpentinite with CO_2-rich fluids. The listwaenite compositions are extremely variable, reflecting the complex reactive genetic process. Formation of listwaenites typically include two major reactive steps, leading to the so-called Stage 1 and Stage 2 or silica-rich Listwaenites (Buckman and Ashley, 2010). Stage 1 Listwaenites mainly consist of carbonate minerals such as dolomite, ankerite, siderite and magnesite, locally associated with relict serpentine. The alkaline earth from serpentinite to Stage 1 Listwanite involves a substantial bulk rock loss of MgO and SiO_2, and corresponds to a volume increase of about 63 % (TuysuzNecati and ErlerAyhan, 1993). Stage 2 listwaenite starts to form when MgO is no more available because of serpentine exhaustion but the CO_2-rich fluid activity is still high. The fluids become acidic and dissolve the carbonates, that are replaced with pure silica (quartz, chalcedony, or opal) releasing CO_2 in solution.

3.3.9. Mining waste and tailings

Mine waste and tailings may also offer an opportunity for *ex situ* storage. The emerging mining industry, particularly in Saudi Arabia and Oman, represents an opportunity to valorize tailings currently considered waste, and favour a circular economy approach. No examples of waste valorisation have been reported in this sense to date in the GCC but the following examples and case studies for similar rocks to those found in the region, highlights feasibility of the approach.

Mine waste rocks were collected from Northern British Columbia, Canada. The selected sample is composed of 65 wt% Olivine, 30 wt% Lizardite and other minor minerals such as 4.2 wt % Magnetite, 1.2 wt % Brucite and 1 wt% Quartz, and has 0.3 wt% CaO, 10.4 wt% Fe_2O_3 and 45.5 wt% MgO. The rocks was tested in 0.1 L stirred autoclave reactor at 185 ˚C and 60 bar for particles on the order of 106 μm with 1 M NaCl and 0.64 M $NaHCO_3$ at a concentration of 150 g/L (Table 2, **Entries 21 and 22)** (Li and Hitch, 2017). A carbonation potential of 15 % was achieved within 0.5 h and increase to 31.7 % within 2 h for a kinetics constant of 0.005 h^{-1} (Li and Hitch, 2017).

Iron mine waste samples sourced from Jerantut (Pahang), which contain Quartz (16 wt%), Magnetite and Hematite (14 wt%) in major amounts, 10–30 wt% plagioclase, and minor Wollastonite, Diopside and Cordierite (total 2–10 wt%), were also analysed. These samples were tested in 0.25 L stirred autoclave reactors at 80 ˚C and 1 bar for particles sizes <63 µm using 1 M NaCl and0.64 M $NaHCO_3$ with 200 g/L sample concentration for 1 h (Table 2, **Entries 23 and 24)** (Kusin et al., 2023). The carbonation conversion of Fe reached 5.32 % and 5.23 % for Ca at pH= 8 while increasing to 5.62 % for Fe and 5.61 % for Ca at pH=12 (Kusin et al., 2023).

3.4. Remarks on minerals and rocks reactivity and prospects

The reactivity of minerals was discussed in terms of conversion of magnesium/calcium/iron silicates in feed materials to magnesium/calcium/iron carbonates. The heterogenous mineralogy of rocks has a major impact on the carbonation potential. The reactivity of different minerals, including polymorphous minerals, will change based on the reaction conditions, and marked chemical modifications may be related to the starting mineral phases (Rasool and Ahmad, 2023).

The carbonation potential was enhanced for Mg and Ca containing minerals and favoured by increasing pressure and temperature conditions that led to faster kinetics, whereas the presence of pH controller additives supported faster dissolution of the rocks and significantly increased the carbonation potential (Park and Fan, 2004). In particular, temperature has a substantial effect, as the high temperature experiments (100, 180 and 200 ˚C) produced much higher Mg, Ca and Fe extraction efficiency than the lower temperature experiments;

raising the reaction temperature, increases reaction and mass transfer rates (Huijgen, Wouter J et al., 2006). At low temperatures, carbonation is rapidly limited by diffusion preventing high conversion degrees (O'Connor et al., 2005).

Pre-treatments performed on Ca/Mg silicates were found to improve reaction kinetics for some potentially attractive Ca/Mg-silicates by activating the mineral for carbonation. Such pre-treatments aim at amorphizing the mineral lattice to create disorder within crystal structure, thus increasing the specific surface area, freeing some of the required cations (e.g., Ca and Mg), and facilitating dissolution (Power et al., 2013). Thermal treatments increase the porosity and the resulting surface area by removing chemically bound water. This treatment is suitable only for Serpentine, which contains up to 13 wt% chemically bound water. The hydroxy groups of Serpentine are removed by heating it to 600–650 °C (Gualtieri et al., 2012). Thermal activation with stream treatment (O'Connor et al., 2002) and microwave treatment (Bobicki, 2014) were also found to act effectively. Chemical activation influences the magnesium silicate structure by polarizing and weaking the magnesium bonds. Various acids and bases, including HCl, HNO_3, H_2SO_4, and NaOH, were used in literature to enhance the dissolution kinetics of minerals and rocks and improve carbonation efficiency (Maroto-Valer et al., 2005a; Sanna et al., 2014; Teir et al., 2007a). For instance, the carbonation efficiency of Olivine reached almost 40 % in 1 h in 0.64 M $NaHCO_3$ solution, while in DI solution at similar conditions the carbonation efficacy was only 27 %. However, the brucite mineral exhibited the opposite effect: aqueous carbonation in 0.5 M HCl solution showed a capture efficacy of 58 % in 2 h, whereas in DI water it was 98 % in 2 h. Analysis of the solution chemistry shows that, as expected, the HCl slurry exhibits higher concentrations of Mg^{2+} compared to DI water throughout the experiments, indicating more extensive dissolution of brucite in the acidic environment. However, charge balance analysis reveals that the concentration of HCO^{3-} in HCl falls below that in DI water after about 2 h. Moreover, the lower pH of the HCl solution results in a reduction of $CO_3{}^{2-}$ concentration by roughly 50 %. Over time, the difference in Mg^{2+} concentration between the two solutions decreases from around 250 % at 15 min to approximately 17 % at 135 min (Zhao et al., 2010). These combined effects may have adversely affected the crystallization of carbonate phases, resulting in a lower extent of carbonation in the HCl solution. Therefore, the addition of acids or bases generally enhances the dissolution of minerals and accelerates reaction kinetics, but this effect is significant only if the reactions are conducted for short periods. If the reaction continues for longer durations (>2 h), the acidic solution may have the opposite effect on the reaction kinetics (Zhao et al., 2010).

In most batch-performed testing, an increase of the solid to liquid (S/L) ratio reduced the dissolution efficiency due to the precipitation of Magnesium-Calcium silicate and to the formation of excess water acting as a transfer barrier, lowering locally the ionic strength of the solution, and resulting in weaker rates of reactive metal cations dissolution (Dri et al., 2014). The use of high S/L ratio would lead to an improved heat balance, due to less energy required heat reactor, reduced size of the reactor and less energy required to pump the slurry (Dri et al., 2014). The carbonation potential was also found to sharply increase for smaller particles distributions for ultramafic rocks, typically obtained by milling (Molahid et al., 2022). This point is critical since the open porosity and tortuosity of the rocks may greatly vary across various geological settings and confirm the impact of rock fracturation as well as available surface area for reactivity during carbonation reactions (Molahid et al., 2022; Wang et al., 2019). The greater surface area would favour reactive metal ions, primarily including Mg^{2+} and Ca^{2+}, and dissolution, ultimately improving the mixing of the boundary layer formed within the pores (Wang et al., 2019). The development of carbon capture at scale through geological carbonation reactions should therefore carefully consider the impact of the materials porosity and fractures on the diffusivity of the gases and brines to reach appropriate rock formation and support the dissolution of the reactive metal ions.

Unfortunately, the reported literature is often partial and several parameters, including the size distribution of the particles, their porosity and homogeneity were nearly systematically absent from reports. In addition, some variability within the analyses may arise from the different reactor geometries, and relative accuracy of the temperatures and pressures used (Romanov et al., 2015). Some tests performed stirred tests, whereas others used static conditions that would also greatly affect the boundary layers at the particle/solution interface, thus equally affecting the dissolution/precipitation kinetics (Kelemen et al., 2019). The development of a matrix of carbonation potential and kinetics performed systematically would support the development of more predictive models to evaluate the relevance of naturally occurring rocks. In addition, the location and depth at which the rocks were extracted are also nearly systematically missing. This is a major issue since the nature of the rocks, their weathering if sourced from a surface location and their level or ageing if extracted from area containing saline aquifers, and the Ca as Mg contents may be greatly affected. Systematic reporting of the localisation of the rocks is therefore required to make any pertinent analysis of the materials performance. The reactivity of minerals and rocks is pivotal in the carbonation process, which involves sequestering carbon dioxide (CO_2) through mineral carbonation. In this process, minerals with high reactivity, containing elements like magnesium (Mg), calcium (Ca), or iron (Fe), readily bond with CO_2 to form stable carbonate minerals such as calcite ($CaCO_3$) or magnesite ($MgCO_3$) (Oconnor et al., 2005). Examples of such reactive minerals include olivine, serpentine, and certain basalts. The reactivity of minerals depends on factors like their chemical composition, crystal structure, and surface area. Rocks, composed of minerals, exhibit varying reactivity based on their mineral composition and overall structure (Hills et al., 2020). Rocks with a higher proportion of reactive minerals tend to exhibit greater carbonation rates, particularly if they possess high porosity and permeability, facilitating enhanced CO_2 diffusion and mineral-fluid interaction for effective carbon capture and storage (Hills et al., 2020).

4. Pilot scale geological CO_2 mineralization plants

The influence of mineral carbonation on a storage location and the rate of mineralization depends on multiple technical factors, including the rock type, pressure, temperature conditions, and the injection methods utilized. Enhancing mineral carbonation can be achieved by introducing carbon dioxide into silicate rocks that are rich in divalent cations (such as Ca^{2+}, $Mg2^{+}$, Fe^{2+}) or by injecting fully dissolved CO_2 in water, as discussed in Section 3. This section details the pilot to full-scale flagship projects for assessing the practicality and effectiveness of geological sequestration through mineral carbonation as a climate change mitigation strategy.

4.1. Sleipner project (Norway)

The Sleipner Project for geological CO_2 fixation was established in October 1996 at Sleipner gas field in the North Sea with high capital investment of $94 million USD (Huo and Jalali, 2010). The Sleipner project was the first commercial application of CO_2 storage in deep saline aquifers in the world (Lindeberg et al., 2009; Torp and Gale, 2004). CO_2 gas obtained from the produced natural gas was separated using an amine-based solvent system, which selectively absorbs CO_2 from the gas stream, and further injected into the sand layer called as the Utsira formation (Torp and Gale, 2004). The total operational expenses, including fuel consumption and CO_2 tax on emissions, amount to approximately $7 million USD per year (Torp and Brown, 2005). Other key components of these expenses included cost for amine solvents and energy used in CO_2 capture, energy and maintenance for CO_2 compression, pipeline operation, and injection and monitoring costs for CO_2 storage. Additionally, general operational costs such as labor and utilities were also included (Kongsjorden et al., 1998) (Gale et al., 2001).

The Utsira formation is a highly elongated sand reservoir, extending for >400 km from north to south and between 50 and 100 km from east to west, with an area of some 26,100 km^2 (Torp and Gale, 2004). The lower cap rock seal of the Utsira formation provides an effective sealing of the CO_2 injected at Sleipner, therefor capillary leakage of CO_2 does not occur in this region (Lindeberg et al., 2009). It was estimated that about 1 million ton of CO_2 is getting stored in the Utsira every year from the Sleipner project (Torp and Gale, 2004). One major challenge of the project is that the Utsira region, the primary site of CO_2 injection, has demonstrated very limited carbonation reactions (Kongsjorden et al., 1998). The reaction of CO_2 mostly occurred with the shell fragments rich in Ca^{+2} ions and silicate minerals to produce carbonates. The shells and silicates are present in trace quantity of only 3–5 % of the overall Utsira (Ahmadinia et al., 2020). Therefore, it is estimated that only up to 5 % mineralization of the injected CO_2 in the Utsira formation occurred, (Kongsjorden et al., 1998).

Several laboratory experiments and simulation data also evaluated the possible reactions occurring between the stored CO_2 and the mineral phases of the Utsira formation and it was confirmed that sand in the Utsira region showed very limited reactions with CO_2 (Kongsjorden et al., 1998). The reaction of CO_2 mostly occurred with the shell fragments rich in Ca^{+2} ions and silicate minerals to produce carbonates. The shells and silicates are present in trace quantity of only 3–5 % of the overall Utsira (Ahmadinia et al., 2020). Therefore, mineralization of the CO_2 in the Utsira formation did not store a significant proportion of the injected CO_2 within the Utsira formation (Kongsjorden et al., 1998). The successes of Sleipner Project include being among the first large-scale implementations of CCS technology, demonstrating the feasibility of capturing and storing CO_2 emissions underground. With an annual capacity to separate and store approximately one million ton of CO_2, Sleipner significantly contributes to reducing greenhouse gas emissions, aligning with Norway's environmental commitments. Moreover, the project has validated the safety and efficacy of geological storage techniques, setting a precedent for similar CCS initiatives worldwide. Despite its achievements, Sleipner faces challenges such as high costs, limited scalability, public scepticism regarding CO_2 storage safety, and evolving regulatory frameworks. To realize its full potential in mitigating carbon emissions, such economic and regulatory shortcomings need to be addressed, while continuing to refine and expand its operational capabilities.

4.2. Wallula pilot plant (USA)

The CO_2 sequestration by natural rocks has been demonstrated at pilot scale near Wallula region in Washington, USA in 2013. The Wallula Pilot Plant's capital expenditure was approximately $73 million USD. This expenditure covered various aspects of the plant's development, including infrastructure, capture equipment, compression facilities. The operational expenditure for the Wallula Pilot Plant, was estimated to be approximately $11 million USD per year associated with capturing, transporting, and storing CO_2, including energy, maintenance, labour, and other operational expenses (Snæbjörnsdóttir et al., 2020).

In the Wallula project, the liquid CO_2 was infused in the basalt rocks in the Columbia river flood and injection of liquid CO_2 was maintained at 40 ton per day (Fig. 2(a)) (McGrail et al., 2014). The CO_2 was liquidized in the Wallula project by consecutive heating of the gas stream followed by pressurization before the infusion with the basalts (McGrail et al., 2017). At the depth of 800–900 m in the river floor, the brecciated basalt zones were identified, and the liquid CO_2 was subsequently injected. The trapping of CO_2 was suspensefully demonstrated by the geological surveys tin the form of free-phase CO_2 in the basaltic cap rock comprising multiple interflow zones (McGrail et al., 2017). A fraction of CO_2 was also mineralized into carbonates (mostly ankerite) in the fractures of basalts, which was confirmed by retrieval and analysis of side-wall cores of basalts after 2 years post CO_2 injection, indicating slow mineralization of CO_2 (Snæbjörnsdóttir et al., 2020). The isotope analysis of the ankerite obtained from the basalt cores confirmed that the parent carbon of these carbonates was from the initial injected CO_2. The elemental analysis of ankerite nodules was performed by Energy-dispersive X-ray spectroscopy, which revealed the elevated presence of Ca, Mg, Mn and Fe, confirming that the elements were from the host basalt in the mineralization process (McGrail et al., 2017). A challenge associated with the project is the lack of quantitative data on the amount of free-phase CO_2 and CO_2 sequestered as carbonates within the pores and fractures of the basalts (McGrail et al., 2017). Explicit and frequent monitoring of surface and pores of the storage basalts over the years confirmed no signs of CO_2 leakage since its injection (Snæbjörnsdóttir et al., 2020). The injection of pressurized liquid CO_2 into the basaltic reservoir in the Wallula project and Wallula pilot borehole are shown in Fig. 2(a) and (b). The Wallula pilot plant has played a pivotal role in advancing CCS technologies, as the field demonstration test involved the injection of 977 t of supercritical CO_2 (scCO2) into two deep basalt brecciated zones in August 2013, nearing 1 million ton/year of CO_2 sequestration. However, there is no quantitative data yet reported to determine the amount of free phase CO_2 and CO_2 sequestered as carbonates in the pores and fractures of basalts. Explicit and frequent monitoring of surface and pores of the storage basalts over the years confirmed no signs of CO_2 leakage since its injection (Snæbjörnsdóttir et al., 2020).

4.3. CarbFix pilot plant (Iceland)

The CarbFix pilot plant demonstrated the *in-situ* carbonation of CO_2 in the basalt rocks at underground CO_2 injection site, about 3 km from Hellisheidi power plant in southwest Iceland in 2012 (Gíslason et al., 2018). The Carbfix Project in Iceland is a leading CCS initiative focused on mineral carbonation. The project's initial capital expenditure was approximately EUR 88 million ($95 million USD) (Ragnheidardottir et al., 2011), covering the construction of capture facilities and CO_2 injection infrastructure while the annual operational expenditures are around $3 million USD, which includes costs for CO_2 capture, compression, transportation, and ongoing maintenance (Snæbjörnsdóttir et al., 2020).

The Hellisheidi power plant produced 160 ton of CO_2 per day and transported to the injection site via pipeline (Ragnheidardottir et al., 2011). The infusion of CO_2 in the basaltic rocks is through the aqueous phase in which CO_2 is first fully dissolved in water, which requires 22 ton of water per ton of CO_2 stored at the CarbFix site. The challenge of injected CO_2 coming back to the surface of rock was actually mitigated by injecting CO_2 charged water to the rocks, since it is denser and also acidic in nature leading to dissolution of divalent cations of basalt for mineralization (Ragnheidardottir et al., 2011). Furthermore, Carbfix does not provide precise details on the water consumption of its method, however it has been estimated that the Carbfix process requires 25 tons of water for the mineralization of one ton of CO_2 (Etcheverry et al., 2021). This means that a large-scale introduction of the Carbfix technology could exacerbate demand not only for energy, but also for water. To apply the Carbfix process in areas with limited water resources, the initiative plans to begin initial trials with seawater in late 2021 and conduct further testing in 2022. However, the project descriptions do not clearly address how the potential risk of saline water re-entering groundwater and impacting drinking water, ecosystems, or agricultural land will be managed on a large scale.

The mineralization reactions of basalt with aqueous CO_2 in Carbfix pilot project is given in Fig. 2 **(C and D)** (Gíslason et al., 2018). As per Henry's raw, high pressure is required for the dissolution of CO_2 in water. In the Carbfix pilot project, maximum efficiency of CO_2 dissolution was achieved by co-injecting CO_2 and local groundwater into the target basalt aquifer as the gas readily dissolves in deeper region due to the existence of higher pressure near the subsurface of basalt at the depth of 1000–1500 ft (Aradóttir et al., 2011). The CO_2 was injected in a separate pipe to a depth of 1500 ft, where it was released into the down-flowing groundwater as small bubbles. The Carbfix technology successfully fixed 12,000 ton of CO_2 in the span of 1 year from 2012 to 13 (Gíslason et al., 2018). Starting from 2017, Carbfix has partnered with Climeworks, a

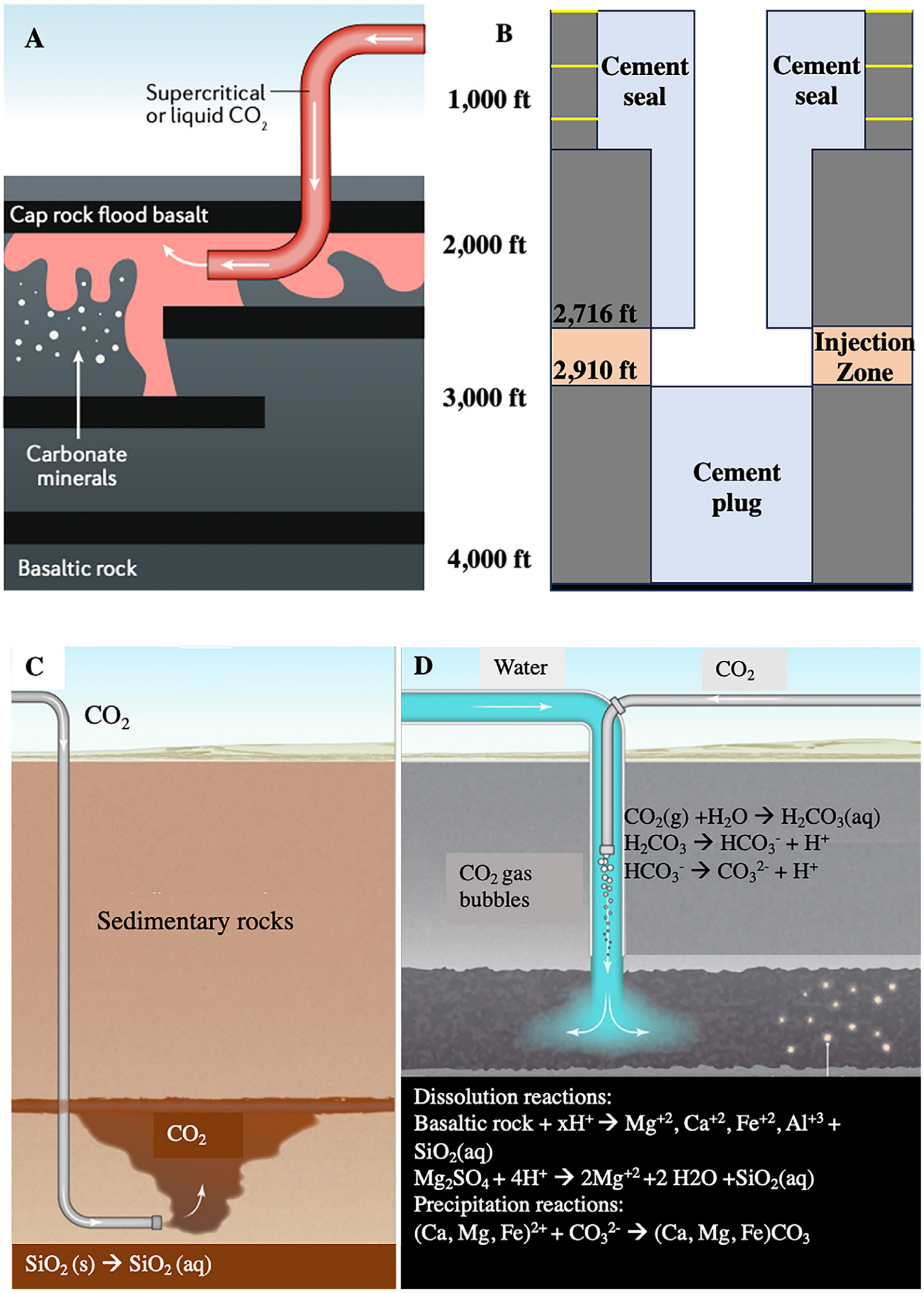

Fig. 2. (A) The injection of pressurized liquid CO_2 into the basaltic reservoir in the Wallula project (reprinted with permission from Nature (Snæbjörnsdóttir et al., 2020)); (B) Wallula pilot borehole (reprinted with permission from Elsevier (McGrail et al., 2014)); (C) The injection of supercritical CO_2 into sedimentary basin with impermeable cap rock (reprinted with permission from Elsevier (Gíslason et al., 2018)); (D) Injection of CO_2-charged water into basaltic rocks at the CarbFix pilot injection site at Hellisheidi, Iceland (reprinted with permission from Elsevier (Gíslason et al., 2018)).

Swiss clean-tech firm focusing on direct air capture (DAC) technology (Yafiee et al., 2024). Their initial joint effort led to the development of a small DAC pilot plant called Arctic Fox, situated alongside Carbfix's CO_2 mineral storage operations at the Hellisheidi geothermal power plant, as part of the EU-funded Carbfix2 project. The power plant provides renewable energy for the DAC process, while Carbfix takes in the captured CO_2, ensuring its secure underground sequestration (Gutknecht et al., 2018).

4.4. *Gorgon project (Australia)*

The Gorgon CO_2 injection Project forms an integral part of the broader Gorgon Project, which revolves around the extraction of natural gas on Barrow Island in Western Australia. Its primary objective is the establishment and operation of facilities designed for capturing and securely storing CO_2 to mitigate the greenhouse gas emissions associated with the overall Gorgon Project with a target of achieving a 40 % reduction. The Gorgon Project in Australia represents a substantial investment in CCS, with capital budget of \$3.5 billion USD, while the operational expenditure for the project is around \$40 million USD per year (Marshall, 2022). When operating at peak capacity, this initiative has the capability to store a maximum of 4 million ton of CO_2 annually. This makes it the world's largest CO_2 sequestration facility and, notably, it boasts the longest operational lifespan, anticipated to exceed 40 years (Flett et al., 2009).

The mechanics of the project involve the extraction of CO_2 from the natural gas stream, followed by its transportation via pipelines to one of three designated drill centers. The pipeline spans a length of 7 km, connecting the liquified natura gas (LNG) plant site to these drill centers. Subsequently, the CO_2 is channeled through nine injection wells that have been directionally drilled from the drill centers. Ultimately, it reaches the Dupuy saline formation (rich in fine grained sandstone and siltstone), located around 2.3 km beneath Barrow Island - an offshore nature reserve, where it is permanently sequestered. The injection project commenced operations in early August 2019. Over its operational lifetime, it is anticipated to sequester >100 million ton of CO_2 (Beckwith, 2011). The Gorgon Project represents a collaborative effort among several key stakeholders, including the Australian subsidiaries of Chevron (47.3 %), ExxonMobil (25 %), Shell (25 %), Osaka Gas (1.25 %), Tokyo Gas (1 %), and JERA (0.417 %) (Flett et al., 2009). In 2020, the Gorgon pilot plant faced significant issues as CO_2 injection averaged only 70 % of its capacity due to malfunctioning water wells, despite having permits from Western Australia's Department of Mining, Industry Regulation and Safety. Chevron's failure to fix these problems led regulators to limit CO2 injection to two-thirds of its capacity starting January 1, 2021, to avoid high pressure and potential leaks. This restriction was anticipated to result in an extra 2.64 million ton of emissions annually (Milne, 2021).

4.5. East bend plant (USA)

The main goal of the East Bend Project was to evaluate the effectiveness of CO_2 storage in the Mount Simon formation (rich in clay, quartz, and feldspar) and gather data to enhance the understanding of regional characteristics such as permeability, porosity, geochemistry, and mineralogy in the Mount Simon Sandstone (Carroll et al., 2013). The East Bend Generating Station project unfolded over a span of about three years, starting in 2006 and was a part of a broader effort to demonstrate and advance CCS technology on a commercial scale. The capital expenditure associated with these efforts were projected to be approximately $600 million USD. This substantial investment covered the costs related to the development and deployment of the sequestration infrastructure and technology. Additionally, the operational expenditures were estimated to be around $10 million USD annually. These ongoing costs encompassed the routine maintenance, monitoring, and management of the CO2 sequestration systems, ensuring their effective and efficient operation throughout the project's lifecycle (Carroll et al., 2013).

The initial assessment of the site indicated favorable conditions within Mount Simon, including sufficient depth, favorable porosity, and permeability, along with overlaying low permeability confining layers to securely contain the injected CO_2. In September 2009, a total of around 910 t (approximately 229,000 gallons) of supercritical CO_2 was injected into Mount Simon over a one-week period at depth of 6500 ft. The injection test achieved a CO_2 injection rate of approximately 5 barrels per minute (bpm), limited by the pumping equipment utilized rather than the injectivity of the formation. This injection rate roughly translates to 1200 t per day or around 0.4 million metric ton per year (Olajire, 2013). A simulation study conducted modeling to replicate the injection of a large quantity of CO_2 (approximately one million ton per year for 100 years) into the Mt. Simon sandstone. It was revealed that most of the injected CO_2 remained concentrated within a lateral distribution radius of 3300 m. The injected CO_2 (within the 0–3300-meter range), caused the formation of a strongly acidified zone with a pH range of 3–5. This led to extensive mineral precipitation and dissolution. The simulations suggested that the prolonged presence of an acidic brine plume, implying that long-term risk assessment should shift from the primary concern of CO_2 leakage to the secondary risk of acidic plume leakage once all the CO_2 has dissolved (Anderson and Jahediesfanjani, 2019; Gupta et al., 2009).

4.6. Concluding remarks on pilot scale geological CO_2 capturing plants

The operational parameters of pilot scale geological CO_2 mineralization plants are summarized in Table 3 for direct comparison purpose. It was concluded that the functioning of pilot scale CO_2 mineralization plants requires high capital cost in the form of injection and monitoring wells. The annual cost of electricity, water and monitoring also add up, which make it extremely costly to scale the plants at commercial level. When implementing CO_2 storage at geological sites on a pilot scale, there are other potential risks and challenges to consider such as leakage due to natural fractures or faults in the geological formation or cap rock, which function as a seal to contain the injected CO_2, leading to environmental and safety hazards. The maintenance of appropriate pressure in the storage reservoir is crucial for safe storage since overpressurization can lead to fractures and leakage, while under pressurization may reduce the storage capacity and effectiveness. CO_2 plumes can migrate within the geological formation, potentially reaching areas with ground/drinking water resources or other sensitive environments, therefore, proper monitoring and modelling are essential to predict and prevent migration. Injection of large amount of CO_2 has potential risks of inducing seismic activity if it increases pore pressure along fault lines. Lastly, compliance with environmental regulations and obtaining necessary permits is critical. Failure to meet regulatory requirements can lead to legal and financial risks. In order to mitigate these risks, pilot-scale CO_2 storage projects typically involve extensive site characterization, monitoring, and modelling efforts, adhering to best practices in well construction, operation, and maintenance.

5. Life cycle assessment of CO_2 sequestration in rocks

The life cycle of mineral carbonation includes several key stages for capturing and storing CO_2 by converting it into stable carbonates (Fig. 3) (Khoo et al., 2011). The process begins with mining the minerals, followed by pre-treatment stages including crushing, grinding, and milling to achieve a particle size of up to 100 μm, which enhances their reactivity. This stage is energy-intensive and produces CO_2 emissions (CO_2(1) as shown in Fig. 3) (Khoo et al., 2021). The processed minerals are then transported to a carbonation facility located near power plants with carbon capture and utilization units. The transportation also requires energy and results in additional CO_2 emissions (CO_2(2), depicted in Fig. 3). Standard carbon capture technology achieves a maximum capture rate of about 90 %, leaving some emissions from the power plants unprocessed, which contributes to CO_2 output (CO_2(3) in Fig. 3) (Digulla and Bringezu, 2023).

In the second phase, CO_2 is captured from the power plant's flue gas using conventional methods such as amine scrubbing, which provides a high recovery rate but involves the use of chemicals such as monoethanolamine (MEA) and further energy consumption (Khoo and Tan, 2006). The third phase involves mineralization, where the captured CO_2 (illustrated as $^*CO_2$ in Fig. 3) is reacted with the prepared minerals under controlled conditions to produce stable carbonate minerals. This step requires the addition of water and acid/base solutions to adjust pH for effective carbonation reactions (Neeraj and Yadav, 2020).

Finally, the produced carbonates undergo further processing to remove impurities, followed by packaging and transportation for sale (Baciocchi and Costa, 2021). This post-processing also requires energy and generates CO_2 emissions (CO_2(4), as shown in Fig. 3). Despite the energy-intensive nature of the process, the resulting carbonates can be sold for $80–110 USD per ton, which may compensate the associated energy costs (Woodall et al., 2019). The mineral carbonation process aligns with the principles of a circular economy, as the total amount of CO_2 captured and converted into carbonates ($^*CO_2$) should exceed the CO_2 emissions generated throughout the entire process.

A reference Life Cycle Assessment (LCA) research by Åbo Akademi University (ÅAU), Finland, focused on several crucial areas: understanding the material and energy needs for sequestering 1 ton of CO_2 in mineral silicate and evaluating the net greenhouse gas (GHG) emission impacts related to CO_2 sequestration using serpentinite mineral to identify key priorities and opportunities for GHG emission reduction was developed (Nduagu et al., 2012). The modelling results indicated a Global Warming Potential (GWP) of 517 kg CO_2 equivalent for every ton of

Table 3
Operational parameters of pilot scale geological CO_2 mineralization plants.

Pilot plant	Geological setting	CAPEX (million USD)	OPEX (million USD/year)	CO_2 Sequestration /Year	Ref
Sleipner Project (Norway)	26,100 km^2 of Utsira formation	94	7	1 million ton	(Gale et al., 2001; Kongsjorden et al., 1998)
Wallula plant (USA)	Basalt rocks of Columbia River flood	73	11	1 million ton	(García del Real and Vishal, 2016; Snæbjörnsdóttir et al., 2020)
CarbFix pilot plant (Iceland)	Basalt in Hellisheidi	95	3	12,000 ton	(Gíslason et al., 2018; Snæbjörnsdóttir et al., 2020)
Gorgon project (Australia)	Barrow Island in Western Australia	3500	40	4 million ton	(Al Kalbani et al., 2023; Marshall, 2022)
East bend plant (USA)	Mount Simon formation	600	10	0.4 million ton	(Carroll et al., 2013; Gupta et al., 2009)

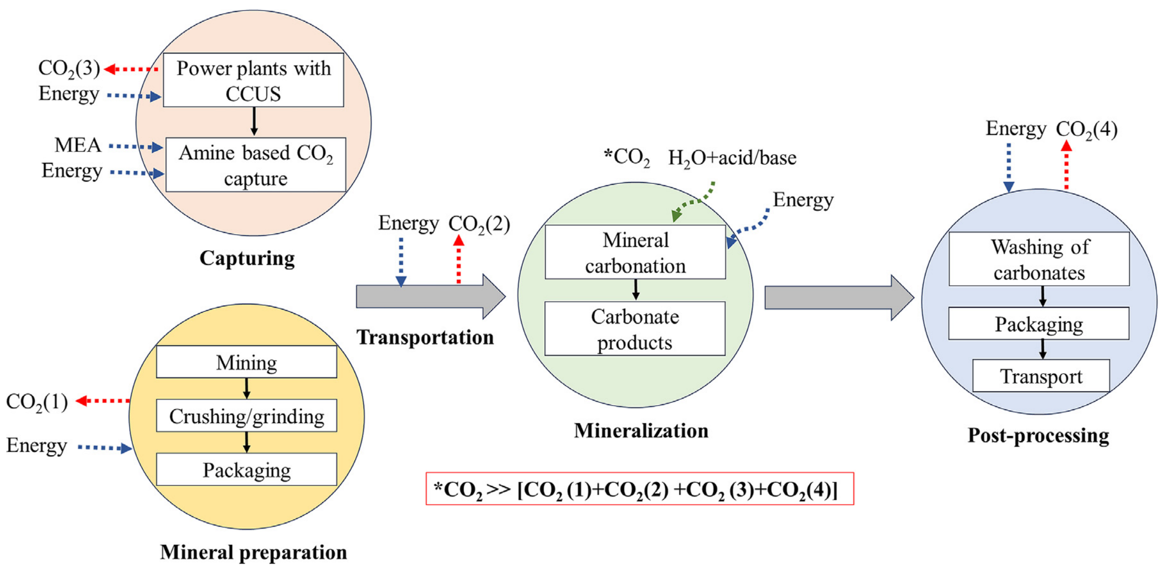

Fig. 3. The life cycle of mineral carbonation involves several stages, beginning with mineral preparation, followed by transportation to a mineral carbonation site near a power plant equipped with CCUS, where an amine-based CO_2 capture unit concentrates the CO_2 gas and directs it to the mineral carbonation process to produce carbonate products. These products are then further processed, packaged, and transported for sale.

CO_2 mineralized in serpentinite (Nduagu et al., 2012), which implies that 483 kg CO_2 can be avoided when 1 ton of CO_2 from a coal power plant is mineralized (Fig. 4(a)). The results were benchmarked with CO_2 mineralization processes of National Energy Technology Laboratory (NETL), US, which showed GWP of 683 kg CO_2, corresponding to 317 kg CO_2 being avoided per ton of CO_2 sequestered (Nduagu et al., 2012). The LCA findings revealed that the ÅAU process has nearly the same energy intensity but a reduced environmental impact compared to the NETL process (Nduagu et al., 2012). Several factors in the ÅAU process contributed to its lower environmental impact, which include the recoverability of the chemical reagent, a lower thermal treatment temperature, achieved at 400 °C enabling the use of nearly emission-free energy sources such as solar thermal energy, as well as heat recovery and/or reduction from power the generation potential of the exothermic gas/solid $Mg(OH)_2$ carbonation reaction (Nduagu et al., 2012). The LCA results from both the ÅAU and NETL processes highlighted that process heat requirements significantly contribute to greenhouse gas (GHG) emissions and that optimizing energy efficiency is crucial for enhancing the net CO_2 sequestration capacity of these processes (Nduagu et al., 2012).

The potential of CO_2 mineralization technology for carbon capture in Singapore using LCA was performed by Khoo and collaborators (Khoo et al., 2021). The study utilized CO_2 flue gas (10 %–15 % (v/v)) from a waste-to-energy plant and serpentine mineral to convert CO_2 into solid carbonates, which was further reutilized for applications such as land reclamation. The findings of the study revealed that in the base scenario when raw material was transported from Australia to Singapore, for every ton of CO_2 input, 937.41 kg CO_2 equivalent was emitted, while 1053.19 kg CO_2 equivalent was abated. This resulted in a net carbon abatement of 115.78 kg CO_2 equivalent per ton of CO_2 equivalent input into the CO_2 mineralization technology (Fig. 4(b)) (Khoo et al., 2021). However, when land transport was excluded from the calculations, 686.76 kg CO_2 equivalent was emitted per ton of CO_2 input. Consequently, the net carbon abatement increased to 366.43 kg CO_2 equivalent. Therefore, carbon emissions from the process were primarily associated with serpentine transportation, thermal activation, and carbon capture, with serpentine transport accounting for nearly half of the total emissions (Khoo et al., 2021). Further examination of ways to enhance carbon abatement potential suggested sourcing serpentine from geographically closer regions to minimize both land and sea transportation. Additionally, recycling waste heat from other industries for the thermal activation process was identified as a viable strategy. The analysis also highlighted that advancements in renewable energy and the electrification of transportation could further enhance the carbon abatement capabilities (Khoo et al., 2021).

The CO_2 recovery from a natural gas combined cycle (NGCC) power plant in Singapore by mineral carbonation using peridotite and serpentinite through a LCA methodology was also evaluated (Khoo et al., 2011). Various simulated scenario was considered by; for the best-case scenario, it was hypothesized that the carbonation process generated

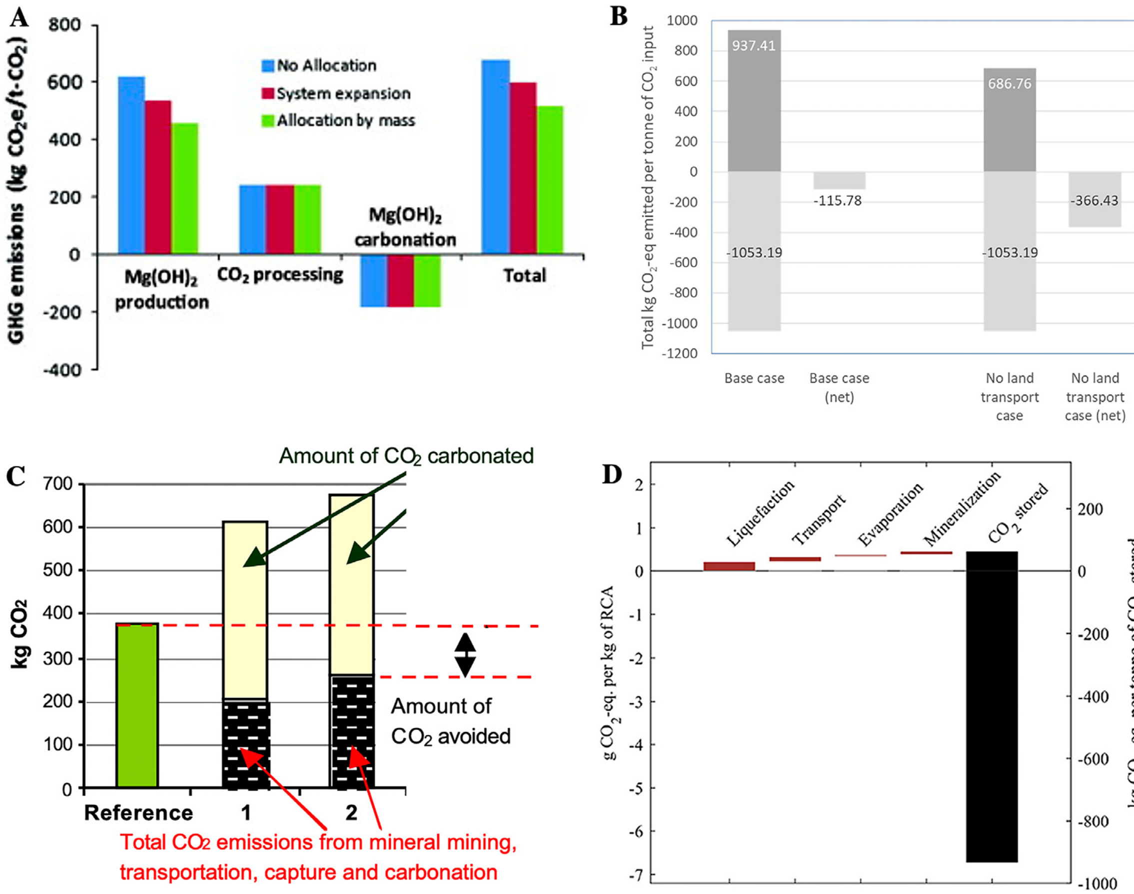

Fig. 4. The greenhouse gas emissions (GHG) throughout the life cycle assessment of (A) Åbo Akademi University process, which includes $Mg(OH)_2$ production, CO_2 processing (involving capture and compression), and $Mg(OH)_2$ carbonation units (Nduagu et al., 2012); (B) CO_2 mineralization technology for CCU in Singapore including transportation constraints (Khoo et al., 2021); (C) NGCC power plant including mineral mining, transportation, capture and carbonation units (Khoo et al., 2021); (D) Biogenic CO_2 capture within concrete aggregates in Switzerland (Tiefenthaler et al., 2021).

enough heat energy to maintain its own operations, leading to an equilibrium in the energy equation and the conversion of minerals into carbonate is assumed to be 90 %. In the worst-case scenario, the heat energy was reclaimed for practical applications leading to high energy requirement for carbonation (up to1,850 MJ/ton of CO_2 carbonated), and the carbonation conversion was limited to 80 %. The CO_2 recovery from the NGCC flue gas led to CO_2 avoidance of 175.2 and 117.6 kg of CO_2 for every 1 MWh of energy generated for optimum scenario, respectively (Fig. 4(c)). The worst-case scenario was less favourable since the benefits of heat recovery were significantly reduced due to the substantial emissions, primarily stemming from energy requirement in carbonation processes (Khoo et al., 2011).

Substantial work on mineralization technology that permanently captures biogenic CO_2 by transforming it into $CaCO_3$ within recycled concrete aggregate (RCA) has been demonstrated in a study in Switzerland (Tiefenthaler et al., 2021). Additionally, LCA highlighted the effectiveness of carbonating RCA with biogenic CO_2 as a reliable method for permanently sequestering CO_2 from the atmosphere. The four stages of the CO_2 emission included in the process were CO_2 liquefaction, transportation, evaporation, and mineralization and the LCA results revealed total of 7.2 g of CO_2 stored / kg of RCA (Fig. 4(d)). The carbon removal efficiency of this process is approximately 93.6 % in Switzerland meaning 6.7 g of CO_2-equivalent can be considered as stored. The remaining 0.5 g of CO_2 stored / kg of RCA compensate for the emissions linked to the process, which include materials and energy consumption (Tiefenthaler et al., 2021).

A LCA study analysing the carbon footprint associated with seven pathways proposed in literature was performed (Ostovari et al., 2020). The first five pathways were related to direct mineralization pathways in a continuous Stirred Tank Reactor (CSTR) operating at 10, 100, 115, and 150 bar, and rotary packed bed (RPB), while the indirect pathways included Abo Academy and Nottingham. The first pathway of mineralization of 1 ton of CO_2 in CSTR at 115 bar using serpentine mineral resulted in 1.15 ton of CO_2 equivalent stored. The emission reduction was achieved through two methods: firstly, by extracting and converting CO_2 from the off-gas (1 ton CO_2 equivalent per ton of CO_2 stored), and secondly, by substituting cement as a by-product, measuring at 0.71 ton CO_2 equivalent per ton of CO_2 stored (Fig. 5(a)) (Ostovari et al., 2020). The other six pathways also achieved a reduction of 1 ton CO_2 equivalent by capturing CO_2 from the off-gas. The credit for substituting cements among various pathways varied from 0.53 (direct) to 1.3 ton (indirect) CO_2 equivalent per ton of stored CO_2 (Fig. 5(a)). This variation in substitution credits arises from differences in product mass, which, in turn, result from diverse feedstock and reaction routes within the pathways (Ostovari et al., 2020). Notably, the substitution credit for indirect pathways consistently exceeds that of the direct pathways due to higher production of SiO_2 in the indirect pathways. The most significant positive contribution towards carbon footprint was observed during the carbonation stage, ranging from 72 kg CO_2 equivalent per ton CO_2 stored (in the direct pathway) to 1175 kg CO_2 equivalent per ton CO_2 stored (in the indirect pathway (Fig. 5(a)). This disparity can be attributed to energy-intensive processes, particularly reagent recov-

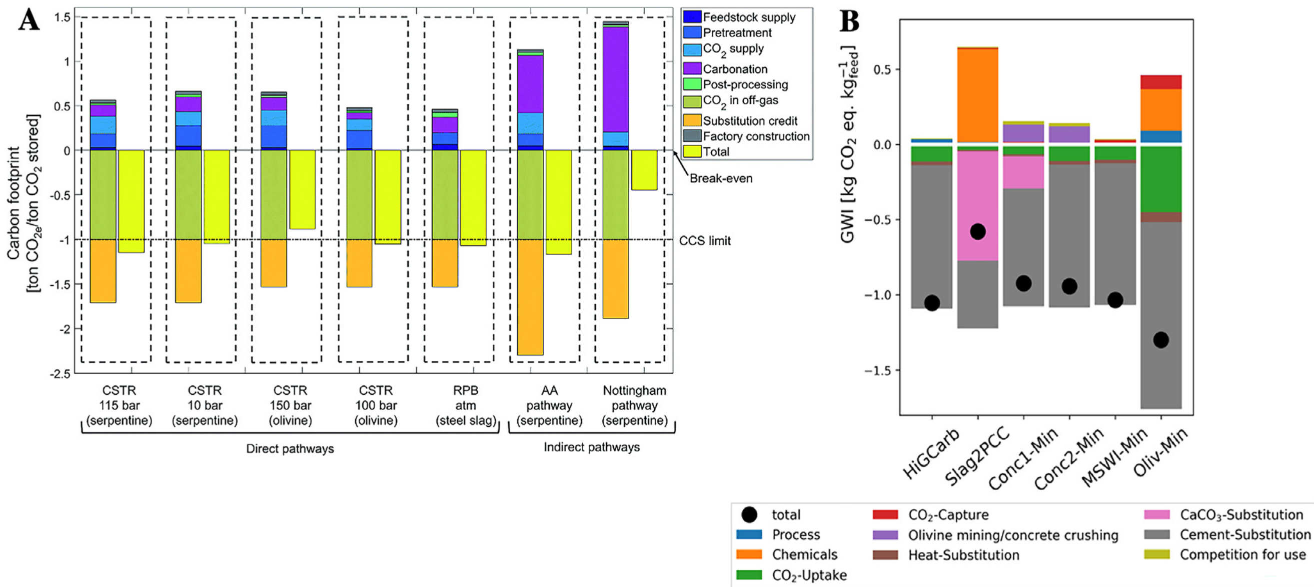

Fig. 5. (A) Carbon footprint associated with 5 direct mineralization pathways in a continuous Stirred Tank Reactor (CSTR) operating at 115 bar, 10 bar, 150 bar 100 bar and rotary packed bed (RPB), and two indirect pathways including Abo Akademi (AA), Finland and Nottingham, UK (Ostovari et al., 2020); (B) Carbon footprint of CO_2 mineralization from production to delivery using various feedstocks such as steel slag, concrete waste, municipal solid waste incineration ash (MSWI), and olivine rock (Digulla and Bringezu, 2023).

ery, which are unique to the indirect pathways. The potential reduction in the carbon footprint could vary from 0.4 to 1.5 Gt CO_2 equivalent per year, which equals 3 % of the global greenhouse gas emissions (Ostovari et al., 2020).

An analysis of CO_2 mineralization assessing the climate and material footprint from production to delivery using various feedstocks such as steel slag, concrete waste, municipal solid waste incineration ash (MSWI), and olivine rock has also been performed (Digulla and Bringezu, 2023). The main findings revealed that the CO_2 reduction footprint ranged from 0.5 to 1.2 kg CO_2 equivalent per kg of feedstock, indicating a decrease in greenhouse gas emissions compared to conventional production methods for respective products (Fig. 5(b)). The olivine mineralization process exhibited the most significant reduction in emissions (1.2 kg CO_2 equivalent per kg of feedstock) due to large CO_2 uptake resulting in large production of cement. Meanwhile, the slag mineralization process showed the weakest reduction (0.5 kg CO_2 e equivalent per kg of feedstock) because of increased process emissions caused by high chemical usage and low CO_2 absorption, the product quantity is consequently lower (Fig. 5(b)) (Digulla and Bringezu, 2023). In the absence of product utilization and functioning solely as carbon capture and storage (CCS) technology, the processes resulted in extremely low GWI values up to 0.01 kg CO_2 equivalent per kg of feedstock. This study underscores the potential of industrial mineralization as a promising technology for mitigating CO_2 emissions (Digulla and Bringezu, 2023).

6. Techno-economic analysis of decarbonization with minerals

One of the major challenges for CCS, including geological mineral carbonation, is to reduce scale-up costs. However, given the lack of currently relevant commercial applications, the forecast costs of mineral carbonation reported are based on laboratory or small pilot scale experiments. The main energy and cost penalties of the process are related to capital investment given the plant size, pre-treatment including grinding feedstock and thermal-treatment, operating conditions and energy-intensive steps including mixing as well as high temperature/pressure, the use of additives to support reactive species extraction or for pH control, and the separation/disposal of the reaction products (Sanna et al., 2014). A comparison of the expenses associated with geological storage and mineral carbonation of CO_2 revealed that geologic storage cost up to US$17–25/ton of CO_2 avoided, while mineral carbonation was estimated at a total of US$81–120/ton of CO_2 avoided (Gielen, 2003) (Fig. 6(a)). The additional costs incurred during mineral carbonation can be rationalized due to the reduction of an extra layer of uncertainty concerning the potential leakage and temporary storage issues inherent to other CO_2 geologic storage methods. The high expenses occurring during mineral carbonation process mitigate risks and provide a secure and predictable approach to long-term CO_2 storage (Sanna et al., 2014).

The sequestration cost of CO_2 into different storage sites such as basin, sedimentary rocks, mafic and ultramafic formations based on the data collected from National Academies of Sciences, Engineering, and Medicine, US was recently analyzed (Kelemen et al., 2019; National Academies of Sciences and Medicine, 2019). The most economical methods for large-capacity CO_2 storage, ranging from US$7–30/ton of CO_2 considering only storage costs, may be achieved through techniques such as supercritical CO_2 injection into subsurface sedimentary formations and *in-situ* carbon mineralization through CO_2-enriched fluid injection into on-land basalt and peridotite formations (Kelemen et al., 2019). Storage in on-land basalt proves competitive with sedimentary reservoirs, although costs increase for seafloor basalts. Several low-cost approaches, including concentrated CO_2 sparging, bioleaching, and stirring, have been developed for CO_2 storage in mine tailings, with costs falling below US$30/ton of CO_2 (Kelemen et al., 2019). *Ex-situ* carbon mineralization ranks among the most expensive methods, with costs typically reaching hundreds of dollars per ton ((Fig. 6(b)), dependent on the reactant and mineralization technique used. Notably, carbonating serpentine-rich and olivine-rich tailings *ex-situ* are more expensive than *in-situ* carbonation of basalt and peridotite due to the expenses related to heating and transportation of the tailings (Kelemen et al., 2019).

The most advanced assessment of *ex-situ* mineral carbonation for CO_2 sequestration costs comes from the extensive work conducted by NETL (Gerdemann, Stephen J. et al., 2007). The process required energy for pre-treatment steps, which involved mining, transportation and crushing and grinding of rocks. Grinding breaks down the mineral particles into smaller sizes improves *ex-situ* mineral carbonation by increasing surface area, accelerating mass transfer and reaction rates. The initial crushing step was calculated to require 2 kWh/ton of en-

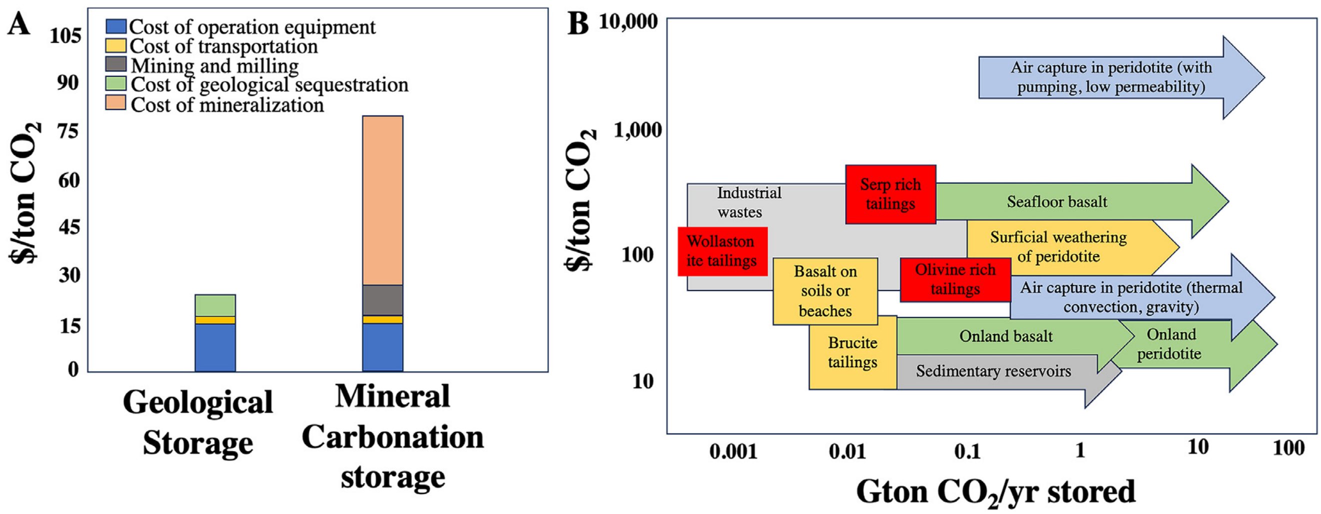

Fig. 6. (A) Comparison of economics of geological and mineral carbonation storage of CO_2 (Gielen, 2003); (B) Overview of CO_2 storage costs (US$/ton CO_2) vs. CO_2 storage capacity per year (Gton CO_2 /year). The red boxes represent costs and rates for *ex-situ* CO_2 mineralization involving heat and concentrated CO_2. Yellow boxes indicate surficial CO_2 mineralization processes, including mine tailings, ground peridotite added to soils or beaches, and peridotite mined and ground for CO_2 removal from air with solid storage. Green arrows signify *in-situ* carbon storage through the injection of CO_2-enriched fluids into mafic and ultramafic formations. Blue arrows depict *in-situ* carbon sequestration by circulating air-saturated water into peridotite formations for CO_2 removal from air with solid storage. The gray arrow represents *in-situ* carbon sequestration by injecting supercritical CO_2 into subsurface sedimentary formations (Kelemen et al., 2019).

Table 4
Techno-economic evaluation of mineralization plants.

Entry	Plant	Minerals	Mineralization Conditions	Extraction agent	Energy consumption (KWh/ton CO_2)	Economic evaluation		Ref.
						Capex (Million US$/ton of CO_2)	OpEx (U$S/ton of CO_2)	
1	NETL, US	Olivine (38–75 µm)	P = 150 Bar, T = 185 °C,	0.64 M $NaHCO_3$, 1 M NaCl	630	–	81	(Gerdemann, Stephen J. et al., 2007)
2	NETL, US	Wollastonite (38–75 µm)	P = 40 Bar, T = 100 °C	DI	429	–	112	(Gerdemann, Stephen J. et al., 2007)
3	NETL	Serpentine (38–75 µm)	P = 115 Bar, T = 155 °C	0.64 M $NaHCO_3$, 1 M NaCl	1008	–	309	(Gerdemann, Stephen J. et al., 2007)
4	Southern Quebec	Serpentinite	P = 20 Bar, T = 25 °C	DI	805	–	144	(Pasquier et al., 2016)
5	Delft, Netherlands	Wollastonite (38 µm)	P = 20 Bar, T = 200 °C	DI	–	45	108	(Huijgen, W. et al., 2007)
6	Delft, Netherlands	Steel Slag (38 µm)	P = 20 Bar, T = 200 °C	DI	–	26	81.6	(Huijgen, W. et al., 2007)
7	DAC-1, Singapore	Olivine (10 µm)	P = 150 Bar, T = 185 °C	DI	1207	2.7	245.0	(Naraharisetti et al., 2019)
8	DAC-2, Singapore	Serpentine (38 µm)	P = 115 Bar, T = 155 °C	DI	552	2.3	176.2	(Naraharisetti et al., 2019)
9	DAC-3, Singapore	Wollastonite (10 µm)	P = 40 Bar, T = 100 °C	DI	808	1.2	253.1	(Naraharisetti et al., 2019)

ergy for all materials and grinding to 75 μm necessitated an additional 11 kWh/ton while subsequent grinding to 38 μm increased costs to a further 70 kWh/ton (Gerdemann, Stephen J. et al., 2007). The energy consumption for the entire sequestration process, including standard pretreatment and carbonation reaction was 630, 429 and 1008 GWh/Mt CO_2 sequestered for olivine, wollastonite, and serpentine, respectively. The sequestration costs for a direct process with pre-treatments were therefore estimated to reach 81, 112, and 309 US$/ton CO_2 avoided for olivine, wollastonite, and serpentine, respectively (Table 4, **Entry 1–3)** (Gerdemann, Stephen J. et al., 2007). The sequestration cost using serpentine was found to be ~3 times higher than the other rocks due to the lower rate of reaction for serpentine (Gerdemann, Stephen J. et al., 2007). The use of serpentinite based mining residues in Southern Quebec, Canada, for mineral carbonation and analysed the energy and economic efficiency of the process to treat raw flue gas emitted from an industrial plant (Pasquier et al., 2016). A model based on a mass balance obtained from laboratory scale experiments allowed the evaluation of the energy requirement of the process. The power consumption reached an optimum of 805 kWh/ton CO_2 when using a train for the rock transportation, biomass for heat activation and hydroelectricity for energy requirements. The estimated process cost amounted to 144 US$/ton CO_2 (Table 4**, Entry 4)** while revenues from the carbonate valorisation reached 644 US$/ton CO_2 generating a net profit considering both the by-product sales and carbon credit recovery. This payback period was only of 1.4 years, making the process promising in terms of financial perspective (Pasquier et al., 2016).

An assessment of the cost of CO_2 sequestration produced in a 100 MW power plant through aqueous mineral carbonation was conducted, utilizing wollastonite and steel slag as feedstock (Table 4**, Entry 5–6)** (Huijgen, W. et al., 2007). The wollastonite carbonation plant showed a total capital expense of 45 million US$. The process equipment was around 11 million USD, with the most expensive components being the grinding equipment (3.1 million US$), compressors (2.5 million US$), reactors (2.2 million US$), and heat exchangers (2.0 million US$) (Huijgen, W. et al., 2007). Meanwhile, the overall capital expenditure was 26 million US$ for steel slag, significantly lower compared to wollastonite, due to of the reduced scale of the operation **(**Table 4**, Entry 5–6)**. The carbonation reactions using wollastonite and steel slag were performed at lower pressure (20 bar), but the reaction temperature was kept at 200 °C, compared to NETL process. The process resulted in the CO_2 sequestration cost of 108 and 81.6 US$/ton CO_2 avoided using wollastonite and steel slag, respectively **(**Table 4**, Entry 5–6)**. For wollastonite, the primary expenses were linked to the feedstock and the electricity requirements for grinding and compression (57 and 28 US$/ton CO_2 avoided, respectively). Besides electricity expenses, the markedly reduced sequestration costs for steel slag were primarily influenced by depreciation and fixed operational costs (24 and 30 US$/ton CO_2 avoided, respectively), owing to the absence of feedstock costs and the smaller scale of the process (Huijgen, W. et al., 2007). Recent advancements in the NETL process have led to an overall mineral carbonation cost of US$90/ ton of CO_2 avoided. This improvement was achieved by using thermal heat instead of electrical energy, along with partial dehydroxylation and heat integration, resulting in a 63 % decrease in the energy requirement for thermal activation.

The analysis of the operational parameters derived from a Direct Aqueous Carbonation (DAC) process for 1 Mton/year mineral processing plant and conducted simulations to assess the factors influencing energy consumption and cost in the CO_2 mineralization process (Naraharisetti et al., 2019). The carbonation reactions were performed using olivine, serpentine and wollastonite particles **(**Table 4**, Entry 7–9)** (Naraharisetti et al., 2019). The mineralization process led to the conversions of 409,200, 368,818 and 285,032 ton/year of CO_2 using olivine, serpentine and wollastonite, respectively. The electricity consumption for CO_2 compression, pumping of slurry water and carbonation was around 60 kWh/ton of mineral and, when combined with the energy needed for grinding, can impose higher electricity burden (from 100 – 250 kWh/ton of mineral) on a power plant supplying electricity to a CCU process. Three DAC scenarios were considered in this study namely DAC-1, DAC-2 and DAC-3 based on different minerals and particle size of minerals used, elaborated in Table 4, **Entry 7–9**. The analysis of different DAC scenarios suggested that the mineral pre-treatment steps, especially intensive grinding, and CO_2 compression consistently emerge as the most significant energy consumers in all scenarios. While smaller mineral particles enable a higher conversion of CO_2 into carbonates, the requirement for intensive grinding down to 10 μm as in case of olivine and wollastonite **(**Table 4**, Entry 7 and 9)** resulted in a higher energy consumption of 1207 and 808 KWh/ton CO_2 captured, compared to serpentine at 38 μm particle size with 552 KWh/ton CO_2 captured **(**Table 4**, Entry 8)** (Naraharisetti et al., 2019). The OpEx for CO_2 mineralization processes were found to range between US$172 (serpentine) to US$253 (wollastonite per ton of CO_2 avoided, including the cost of pure CO_2 at US$70/ton and ore at US$10/ton. The OpEx linked to the CO_2 mineralization process, such as heat and electricity, are relatively lower, ranging from US$31 to US$75 per tonne of CO_2 captured (Naraharisetti et al., 2019).

A thorough investigation to minimizing the usage of chemicals and enhancing carbonation efficiency and product purity is yet to be conducted. Employing indirect aqueous carbonation to produce high-purity products such as precipitated calcium carbonate or hydromagnesite from slags or serpentine necessitates the usage of pH adjusters such as HCl, HNO_3, CH_3COOH, NaOH at a cost ranging from US$600 to US$4500/ton of CO_2 if not regenerated (Teir et al., 2007a). Acid or base assisted carbonation require substantial amounts of HCl/HNO_3 (2–4 ton/ton of stored CO_2) and NaOH (2.4 ton/ton of stored CO_2) to achieve up to 80–90 % CO_2 conversion. The HCl based process costs around US$1300/ton of CO_2, while NaOH cost around US$1100/ton of CO_2. Regenerating the pH adjuster chemicals would emit 2.6–3.5 times the amount of CO_2 captured during the carbonation process (Teir et al., 2007a). Addressing the challenges of the acid/base assisted mineral carbonation process, various techniques have been explored to lower its expenses. Mechanical activation, particularly in the case of Olivine, was found to stand out as an efficient method to accelerate the carbonation reaction but requires significant energy penalty as discussed previously (Arce et al., 2017). A study performed the energy and cost modelling of mechanical activation integrated with mineral carbonation using forsterite and lizardite rich mine waste rocks at Turnagain Nickel project, British Colombia, Canada (Li and Hitch, 2018). The electricity consumption of the integrated process was estimated around 570 KWh/ton of mineral ore and cost came around 104.1–107.1 US$/ton of CO_2 avoided. Despite the substantial costs associated with the integrated mineral carbonation process at Turnagain Nickel plant, the plant was engineered to capture up to 14.62 million ton of CO_2 annually (Li and Hitch, 2018).

Overall, the development of carbonation processes and permanent storage of CO_2 by mineralization and carbonation was demonstrated at scale and represents an opportunity to reduce the carbon footprint of CO_2 emitting processes. The technologies are mature and offer substantial benefits compared to other storage strategies provided that the geological setting is adequate both in terms of composition and interconnected porosity, to allow fast kinetics of reactions within the pores of the rocks.

6.1. SWOT analysis of geological mineral carbonation process

The strengths of the geological mineral carbonation process include its ability to offer a stable and long-term solution for CO_2 sequestration, significantly lowering the risk of leakage compared to other CO_2 storage methods such as geological storage in saline aquifers. An investigation of CO_2 leakage from a deep saline aquifer was conducted using pressure tomography. The findings indicated that CO_2 migrated upward through both a permeable seal and a leaky pathway, achieving saturation levels of 0.62 and 0.86, respectively, in the overlying aquifer. In some instances, CO_2 plumes were also observed in the upper aquifer due to prolonged injection and leakage through these pathways (Hu et al., 2016). Furthermore, the mineral carbonation processes are well-developed and have been demonstrated at lab and pilot scale, indicating their effectiveness for large-scale CO_2 reduction.

The weaknesses include the high cost as mineral carbonation is significantly more expensive compared to other CO_2 storage methods. Costs for mineral carbonation range from $81–120 per ton of CO_2 avoided, while geological storage costs between $17–25 per ton. The process of mineral carbonation requires substantial energy for milling, pre-treatment (crushing and grinding), mixing, pH adjustments and maintaining high temperature and pressure conditions leading to increased cost. Moreover, the range of incurred cost during mineral carbonation can be wide depending on the country specific logistics as well as the type of minerals used for the process. For instance, since olivine and serpentine are less reactive than wollastonite, the energy required for carbonating olivine and serpentine is significantly higher – up to 630 and 1008 GWh/Mt CO_2 sequestered, respectively compared to wollastonite, which requires 406 GWh/Mt CO2 sequestered (Gerdemann, Stephen J. et al., 2007). The lack of large-scale commercial applications further complicates cost forecasting.

Current understanding of the process reveals several possibilities and opportunities for exploration. Advances in technology and process optimization, such as utilizing thermal heaters or emission-free solar thermal energy instead of electrical energy could be a cost-efficient strategy. For instance, using heat from thermal heaters instead of electrical energy, along with partial dihydroxylation of minerals such a serpentine cuts energy requirements for thermal activation by 63 % and lowers the overall cost of the process to about $50 per ton of CO_2 avoided. This is significantly less than the $140 per ton of CO_2 avoided in the NETL process (Wang et al., 2021). Improving heat recovery and employing high-performance biphasic solvents (monoamine + diethylethanolamine solution), for CO_2 capture can lead to an increase in power generation efficiency from 31 % $_{HHV}$ with a conventional MEA system to 38 % $_{HHV}$ with an advanced biphasic solvent and heat recovery (Bui et al., 2018).Furthermore, support from government policies and carbon credits can provide financial incentives to offset high costs and encourage further investment in mineral carbonation technologies.

The threats of the process involve high initial capital investment (>$50 million USD) required for infrastructure, including mining, transportation, and processing equipment, poses a significant financial barrier. Moreover, the energy required for processing and transportation may offset some of the environmental benefits as the amount of CO_2 emitted during the pre-treatment steps can be very high up to 200–250 kgCO_2/ton of processed minerals (Khoo et al., 2021). Additionally, the use of chemicals in acid/base-assisted carbonation processes can result in additional CO_2 emissions if not managed properly. On-site recovery of the acid and base is possible but requires substantial energy. As a result, organic acids such as orthophosphoric acid and oxalic acid have been explored for the carbonation of olivine. This approach has led to a 21 % reduction in mineralization costs while maintaining a similar carbonation efficiency of 0.6 g_{CO2}/g of mineral (Galina et al., 2023; Park et al., 2003).Other carbon capture and storage methods, such as geological storage, may offer more cost-effective solutions or quicker deployment, potentially limiting the adoption of mineral carbonation.

This SWOT analysis highlights the complex balance between the advantages and challenges of mineral carbonation in CO_2 sequestration, emphasizing the need for continued research, technological advancement, and financial incentives to address the high costs and scalability issues associated with this promising method.

7. Legal environment and incentives for CCUS in the MENA region

The MENA region, historically synonymous with oil wealth, is increasingly becoming a focal point in the global transition towards cleaner energy (Dziejarski et al., 2023). This shift includes a significant emphasis on Carbon Capture Utilisation and Storage (CCUS) as a crucial technology for mitigating climate change. The legal environment governing CCUS in the MENA region is complex and varies significantly country-to-country across the region. This section will explore the existing legal frameworks, the regional differences in climate targets, and the carbon credit and tax incentive schemes in place (Dziejarski et al., 2023).

7.1. General progress of the legal framework for CCUS in the MENA region

The MENA region's incentives often come in the form of direct investments by governments and state-owned enterprises, such as ADNOC in the UAE and Saudi Aramco in Saudi Arabia, are leading substantial investments in CCUS projects (Ian Havercroft, 2023). These direct investments are typically focused on large-scale projects that align with national climate goals. In addition, a number of Public-Private Partnerships (PPPs) are frequently used to finance CCUS initiatives. Saudi Arabia's Carbon Management Initiative involves both public and private sector investments. Although no major frameworks have bene developed or implemented in North Africa, several initiatives have been initiated led by UAE and Saudi investment funds have however been initiated in Egypt, Morrocco and Algeria specifically since the mid (Ian Havercroft, 2023).

Saudi Arabia has been proactive in integrating CCUS into its broader climate strategy. The country's approach is primarily influenced by its Vision 2030, which aims to diversify its economy and reduce its dependence on oil. Although in 2021, Saudi Arabia established the Saudi Carbon Management Initiative to advance CCUS technologies, the regulatory framework governing CCUS in Saudi Arabia is still in its developmental stages (Vikram Vishal, 2024). Saudi Arabia 's environmental regulations are overseen by the Saudi Arabian Environmental Protection Agency (EPA) and specific regulations on CCUS are limited, with the focus being more on general environmental protection and emissions standards. Saudi Arabia has engaged in international partnerships, such as its collaboration with the International Energy Agency (IEA) and participation in the Clean Energy Ministerial (IEF, 2024a; Vikram Vishal, 2024). These collaborations influence the regulatory development, incorporating best practices from global standards. Saudi Arabia aims to reduce its carbon intensity by 60 % by 2030 and achieve net zero emissions by 2060. The country's strategy includes substantial investment in CCUS technologies to meet these goals (IEF, 2024a).

The UAE has emerged as a leader in CCUS in the MENA region with a legal framework reflecting the ambition to be a global hub for clean energy. The UAE has developed specific regulations for CCUS, particularly within its free zones, such as Masdar City in Abu Dhabi (IEF, 2024a; Necibi et al., 2022). The Abu Dhabi National Oil Company (ADNOC) is spearheading CCUS initiatives, supported by the UAE's regulatory framework that includes provisions for storage licenses and monitoring requirements. In addition, the UAE's National Climate Change Plan 2050 outlines ambitious targets for reducing greenhouse gas emissions and integrating CCUS. The country aims to capture 5 million tonnes of CO_2 annually by 2030. The UAE's Federal Law No 24 of 1999 on the Protection and Development of the Environment is the primary legislation guiding environmental practices, including CCUS and is complemented by various emirate-level regulations and initiatives. The UAE has set a target to reduce emissions by 70 % by 2030 and achieve net zero by 2050 with significant investment in clean energy technologies (IEF, 2024b).

Qatar, another major oil and gas producer, is making strides in CCUS technology with major CCUS projects, such as the Al-Khaleej Carbon Capture Project. The regulatory environment includes provisions for CCUS in its broader environmental and energy policies, but specific legislation dedicated solely to CCUS is still evolving and is directed by Qatar's National Vision 2030 that includes targets for sustainable development and reducing carbon emissions. Although specific CCUS regulations are not yet fully developed, the strategic focus supports the integration of CCUS technologies (Hafner et al., 2023). Qatar has partnered with international entities and invested in CCUS research, influencing its regulatory approach by incorporating global best practices. Qatar aims to reduce emissions intensity by 25 % by 2030 to be achieved by integrating greener solutions and process optimization for its oil and gas sector (IEF, 2024a, b).

Kuwait's approach to CCUS is more nascent compared to its Gulf neighbours but has been establishing a regulatory framework for CCUS since 2020 (IEF, 2024b). The focus is currently on studying the feasibility and economic implications of CCUS technologies. In addition, Kuwait's National Climate Change Action Plan outlines its commitment to reducing greenhouse gas emissions, but specific CCUS targets and regulations are still under development. Oman is also advancing its CCUS agenda, with particular emphasis on its potential in enhanced oil recovery. Oman's regulatory environment for CCUS is evolving, with the Ministry of Environment and Climate Affairs taking a lead role in integrating CCUS into national environmental policies. Oman's Vision 2040 includes goals for sustainability and reducing carbon emissions, aligning with its CCUS initiatives. The country is focusing on developing regulatory frameworks that support these objectives. Both Kuwait and Oman countries have set broader climate goals, with Kuwait focusing on reducing carbon emissions and Oman targeting sustainability and emissions reduction through its Vision 2040 (IEF, 2024a, b).

As a comparison point with other CCUS policy active blocks, the European Union, Japan, and the United States each employ distinct financial mechanisms, carbon credit systems, and tax incentives to promote and advance CCUS (Truong et al., 2024). Understanding these differences may help drive global policy alignment and provides insight into how regional policies shape the adoption of CCUS technologies. In the MENA region, financial incentives for CCUS are evolving but are generally less mature compared to Europe, Japan, and the United States.

Europe has a well-established framework for financial incentives for CCUS projects through programs such as Horizon Europe and the Innovation Fund. These funds support research, development, and large-scale deployment of CCUS technologies (Dütschke and Duscha, 2022). Countries such as the UK, Norway, and the Netherlands offer national grants and low-interest loans specifically for CCUS projects. The UK's CCS Infrastructure Fund provides up to £1 billion for infrastructure development. Japan offers substantial subsidies for CCUS projects through its Ministry of the Environment and the Ministry of Economy, Trade, and Industry (METI) (Machado e Silva and Costa, 2021). These subsidies support both research and the deployment of CCUS technologies. Japanese corporations, in collaboration with the government, invest heavily in CCUS projects, often leveraging subsidies to reduce financial risk. The U.S. offers a diverse range of financial incentives ranging from Federal initiatives to state level incentives. Programs such as the Department of Energy's (DOE) CCUS initiative and the Infrastructure Investment and Jobs Act, the U.S. provides significant funding for CCUS research and development, while various states offer additional financial support for CCUS, including grants and subsidies for pilot projects and large-scale implementations (Dütschke and Duscha, 2022).

7.2. Carbon credits and financial incentives in the MENA region

Carbon credits and tax incentives are key components in encouraging CCUS investment globally. Most MENA countries are part of international climate agreements, such as the Paris Agreement, which influence their domestic policies on carbon credits and incentives (IEA, 2023). The MENA region is developing carbon credit markets, with the UAE and Saudi Arabia leading in this area. The UAE has established a carbon trading platform, while Saudi Arabia is exploring similar mechanisms. These credits incentivize CCUS projects by allowing companies to earn credits for captured carbon. The UAE offer tax incentives and subsidies for clean energy projects, including CCUS (IEA, 2023). These incentives are designed to attract investment and support the development of CCUS technologies. Much of the carbon credit activity is however in the voluntary market, as regulatory frameworks for mandatory carbon trading systems are still under development. In terms of carbon credits across other blocks, Europe has one of the most developed carbon credit systems with the European Union Emission Trading Scheme (EU ETS) that is a cap-and-trade system that allows companies to buy and sell emission allowances. CCUS projects can generate carbon credits that can be sold or used to offset emissions. In addition, the EU supports various carbon offset projects, including those related to CCUS, through its carbon market mechanisms. Japan's carbon credit system includes the Japan's Emissions Trading Scheme (ETS) that includes carbon credits for CCUS projects (Wakabayashi and Kimura, 2018). The scheme operates alongside the Tokyo Cap-and-Trade Program, as well as the carbon offset programs, allowing Japanese companies to invest in CCUS projects abroad to meet their emissions reduction targets. The U.S. carbon credit system is complex and multifaceted with a mix of federal and state-level carbon trading systems. The California Cap-and-Trade Program and the Regional Greenhouse Gas Initiative (RGGI) are examples where CCUS projects can generate carbon credits. In addition, to regulatory markets, the U.S. has active voluntary carbon markets where businesses can purchase credits from CCUS projects (IEA, 2023).

Tax incentives for CCUS in the MENA region are however less developed than European, American or Japanese ones due to the fact that tax laws in most MENA region are very laxed and limited. The region's tax incentives are generally limited to broad economic policies rather than specific CCUS-related tax breaks. However, some countries offer indirect incentives through broader energy or environmental tax policies. In lieu of direct tax incentives, countries in the MENA region often rely on subsidies and grants to support CCUS initiatives. There are also no fixed carbon pricing, as opposed to European countries, the U.S. or Japan (IEA, 2023; IEF, 2024a).

7.3. Concluding remarks on the legal framework of CCUS in MENA region

The legal environment for CCUS in the MENA region is evolving, with varying degrees of regulatory development across the region. While some countries like the UAE and Saudi Arabia have established more comprehensive frameworks and ambitious targets, others are still in the developmental phase. The incentives for CCUS technologies vary significantly across the MENA region, Europe, Japan, and the United States. As the MENA region continues to diversify its energy portfolio and address climate change, the evolution of its CCUS legal frameworks will play a crucial role in shaping its environmental and economic future.

8. Conclusions and prospects

This study highlighted prospects for CO_2 geo-sequestration within the Middle East geological setting and discussed the potential of various rocks and minerals for long-term carbon capture. The carbonation mechanisms were discussed in terms of scalability and challenges related to both geoscience, and chemical reactors. The techno-economic analysis of integrated mineral carbonation shows great potential for commercialization, especially when the carbonate product can be utilized. The scale of carbon credits generated through a balance between captured CO_2 and CO_2 emissions from the carbonation process may be a way to apply mineral carbonation on a large scale and make it economically feasible.

Although the method offers a practical and convenient pathway to the long-term storage of CO_2, it is only valid in specific geological settings. Access to suitable reactive minerals is therefore major concern, as limited availability in some regions could impede scalability. The kinetics of the reactions are yet slow due to the lack of porosity of most geological settings, reducing the amount of potentially dissolved cations used for the carbonate formation. This aspect strongly reduces the scalability and has impact trials in terms of maximum capture capacity and economics. In addition, unless rock/mineral mining is performed, the formed carbonates will not be available for further utilisation since stored in complex and deep underground settings. Routes to tackle these challenges, and to both increase kinetics and make value out of the produced carbonates in civil engineering applications, may be to selectively mine the proper minerals to extract the relevant ions and react them with CO_2. Current mineral carbonation technology for CO_2 capture and storage encounters several other hurdles that hinder its widespread adoption and efficacy. These challenges include the high costs associated with energy-intensive processes such as rock or mineral crushing and the need for extensive infrastructure. While the market for carbonates and other products from geological sequestration is growing, precise figures on its size may be subject to change and influenced by factors such as technological advancements, regulatory policies, and economic conditions. Furthermore, processes should be improved to reduce the involved costs significantly.

Declaration of competing interest

The authors declare that they have no known competing financial interests or personal relationships that could have appeared to influence the work reported in this paper.

CRediT authorship contribution statement

Priyanka Kumari: Writing – original draft, Validation, Methodology, Data curation, Conceptualization. **Rihab Yahmadi:** Writing – original draft, Data curation. **Fatima Mumtaz:** Writing – review & editing, Writing – original draft, Investigation, Formal analysis. **Lourdes F. Vega:** Writing – review & editing, Formal analysis. **Andrea Ceriani:** Writing – review & editing, Supervision. **Riccardo Tribuzio:** Writing – review & editing, Formal analysis. **Ludovic F. Dumée:** Writing – review & editing, Writing – original draft, Supervision, Formal analysis, Conceptualization. **Alessandro Decarlis:** Writing – review & editing, Supervision.

Acknowledgment

The authors acknowledge financial support from Khalifa University to the Research and Innovation Center on CO_2 and Hydrogen (RICH), project RC2-2019-007, as well as the Decarbonization theme within the Research Center on 2D Nanomaterials (RIC2D).

References

Ahmadinia, M., Shariatipour, S.M., Andersen, O., Nobakht, B., 2020. Quantitative evaluation of the joint effect of uncertain parameters in CO2 storage in the Sleipner project, using data-driven models. Int. J. Greenhouse Gas Control 103, 103180. doi:10.1016/j.ijggc.2020.103180.

Al Kalbani, M., Serati, M., Hofmann, H., Bore, T., 2023. A comprehensive review of enhanced *in-situ* CO2 mineralisation in Australia and New Zealand. Int. J. Coal. Geol. 276, 104316. doi:10.1016/j.coal.2023.104316.

Alhejji, S., Kent, A., Duncan, R.A., Graham, D.W., Al-Amri, A.M., Alshaltoni, S.A., 2019. Geochronology and geochemistry of volcanism at Harrat Ithnayn, Western Saudi Arabia. In: AGU Fall Meeting Abstracts, pp. V11E–0135.

Ali, M.Y., Watts, A.B., Searle, M.P., Keats, B., Pilia, S., Ambrose, T., 2020. Geophysical imaging of ophiolite structure in the United Arab Emirates. Nat. Commun. 11 (1), 2671. doi:10.1038/s41467-020-16521-0.

Anderson, S.T., Jahediesfanjani, H., 2019. Estimating the pressure-limited dynamic capacity and costs of basin-scale CO2 storage in a saline formation. Int. J.Greenhouse Gas Control 88, 156–167. doi:10.1016/j.ijggc.2019.05.031.

Aradóttir, E.S., Sigurdardóttir, H., Sigfússon, B., Gunnlaugsson, E., 2011. CarbFix: a CCS pilot project imitating and accelerating natural CO2 sequestration. Greenhouse Gases: Sci. Technol. 1 (2), 105–118.

Arce, G.L.A.F., Soares Neto, T.G., Ávila, I., Luna, C.M.R., Carvalho, J.A., 2017. Leaching optimization of mining wastes with lizardite and brucite contents for use in indirect mineral carbonation through the pH swing method. J. Clean. Prod. 141, 1324–1336. doi:10.1016/j.jclepro.2016.09.204.

Babamohammadi, S., Shamiri, A., Aroua, M.K., 2015. A review of CO2 capture by absorption in ionic liquid-based solvents. Rev. Chem. Eng. 31 (4), 383–412. doi:10.1515/revce-2014-0032.

Baciocchi, R., Costa, G., 2021. CO2 utilization and long-term storage in useful mineral products by carbonation of alkaline feedstocks. Front. Energy Res. 9. doi:10.3389/fenrg.2021.592600.

Bałdyga, J., Henczka, M., Sokolnicka, K., 2010. Utilization of carbon dioxide by chemically accelerated mineral carbonation. Mater. Lett. 64 (6), 702–704. doi:10.1016/j.matlet.2009.12.043.

Beckwith, R., 2011. Carbon capture and storage: a mixed review. J. Petrol. Technol. 63 (05), 42–45. doi:10.2118/0511-0042-jpt.

Bobicki, E.R., 2014. Pre-treatment of ultramafic nickel ores for improved mineral carbon sequestration.

Bodénan, F., Bourgeois, F., Petiot, C., Augé, T., Bonfils, B., Julcour-Lebigue, C., Guyot, F., Boukary, A., Tremosa, J., Lassin, A., Gaucher, E.C., Chiquet, P., 2014. Ex situ mineral carbonation for CO2 mitigation: evaluation of mining waste resources, aqueous carbonation processability and life cycle assessment (Carmex project). Miner. Eng. 59, 52–63. doi:10.1016/j.mineng.2014.01.011.

Buckman, S., Ashley, P., 2010. Silica-carbonate (listwanites) related gold mineralisation associated with epithermal alteration of serpentinite bodies.

Bui, M., Fajardy, M., Mac Dowell, N., 2018. Bio-energy with carbon capture and storage (BECCS): opportunities for performance improvement. Fuel 213, 164–175. doi:10.1016/j.fuel.2017.10.100.

Camp, V.E., Roobol, M.J., 1992. Upwelling asthenosphere beneath western Arabia and its regional implications. J. Geophys. Res.: Solid Earth 97 (B11), 15255–15271. doi:10.1029/92JB00943.

Carroll, S.A., McNab, W.W., Dai, Z., Torres, S.C., 2013. Reactivity of mount simon sandstone and the Eau claire shale under CO2 storage conditions. Environ. Sci. Technol. 47 (1), 252–261. doi:10.1021/es301269k.

Chorowicz, J., 2005. The east African rift system. J. Afr. Earth Sci. 43 (1–3), 379–410.

Clark Jr., S.P., 1966. Handbook of Physical Constants. Geological Society of America doi:10.1130/mem97.

Cochran, J.R., 2005. Northern Red Sea: nucleation of an oceanic spreading center within a continental rift. Geochem., Geophys., Geosyst. 6 (3). doi:10.1029/2004GC000826.

Daval, D., Martinez, I., Corvisier, J., Findling, N., Goffé, B., Guyot, F., 2009. Carbonation of Ca-bearing silicates, the case of wollastonite: experimental investigations and kinetic modeling. Chem. Geol. 265 (1), 63–78. doi:10.1016/j.chemgeo.2009.01.022.

De Silva, G.P.D., Ranjith, P.G., Perera, M.S.A., 2015. Geochemical aspects of CO2 sequestration in deep saline aquifers: a review. Fuel 155, 128–143. doi:10.1016/j.fuel.2015.03.045.

Digulla, F.E., Bringezu, S., 2023. Comparative life cycle assessment of carbon dioxide mineralization using industrial waste as feedstock to produce cement substitutes. Energies. (Basel) 16 (10), 4118.

Dilek, Y., 2003. Ophiolite Concept and its Evolution. Geological Society of America, p. 373. doi:10.1130/0-8137-2373-6.1 Special Paper of the.

Downs, D.T., Robinson, J.E., Stelten, M.E., Champion, D.E., Dietterich, H.R., Sisson, T.W., Zahran, H., Hassan, K., Shawali, J., 2019. Geologic Map of the Northern Harrat Rahat Volcanic field, Kingdom of Saudi Arabia. US Department of the Interior, US Geological Survey Reston, VA, USA.

Dri, M., Sanna, A., Maroto-Valer, M.M., 2014. Mineral carbonation from metal wastes: effect of solid to liquid ratio on the efficiency and characterization of carbonated products. Appl. Energy 113, 515–523. doi:10.1016/j.apenergy.2013.07.064.

Dumée, L., Scholes, C., Stevens, G., Kentish, S., 2012. Purification of aqueous amine solvents used in post combustion CO2 capture: a review. Int. J Greenhouse Gas Control 10, 443–455. doi:10.1016/j.ijggc.2012.07.005.

Dütschke, E., Duscha, V., 2022. Is there a future for CCUS in Europe? An analysis of the policy framework and societal support. In: Proceedings of the 16th Greenhouse Gas Control Technologies Conference (GHGT-16), pp. 23–24.

Dziejarski, B., Krzyżyńska, R., Andersson, K., 2023. Current status of carbon capture, utilization, and storage technologies in the global economy: a survey of technical assessment. Fuel 342, 127776. doi:10.1016/j.fuel.2023.127776.

Etcheverry, M.P., Yu, H., Gençer, E., 2021. Techno-economic evaluation of Carbfix technology for carbon storage in the US. In: Türkay, M., Gani, R. (Eds.), Computer Aided Chemical Engineering. Elsevier, pp. 365–371. doi:10.1016/B978-0-323-88506-5.50058-9.

Flett, M., Brantjes, J., Gurton, R., McKenna, J., Tankersley, T., Trupp, M., 2009. Subsurface development of CO2 disposal for the gorgon project. Energy Procedia 1 (1), 3031–3038. doi:10.1016/j.egypro.2009.02.081.

Gale, J., Christensen, N.P., Cutler, A., Torp, T.A., 2001. Demonstrating the potential for geological storage of CO2: the sleipner and GESTCO projects. Environ. Geosci. 8 (3), 160–165. doi:10.1046/j.1526-0984.2001.008003160.x.

Galina, N.R., Arce, G.L.A.F., Maroto-Valer, M., Ávila, I., 2023. Experimental study on mineral dissolution and carbonation efficiency applied to pH-swing mineral carbonation for improved CO2 sequestration. Energies. (Basel) 16 (5), 2449.

García del Real, P., Vishal, V., 2016. Mineral carbonation in ultramafic and basaltic rocks. In: Vishal, V., Singh, T.N. (Eds.), Geologic Carbon Sequestration: Understanding Reservoir Behavior. Springer International Publishing, Cham, pp. 213–229. doi:10.1007/978-3-319-27019-7_11.

Gerdemann, S.J., Dahlin, D.C., O'Connor, W.K., Penner, L.R., Rush, G.E., 2004. Ex-situ and *in-situ* mineral carbonation as a means to sequester carbon dioxide. In: Conference: 21st Annual International Pittsburgh Coal Conference. Osaka, Japan Sept. 13-17, 2004 Related Information: Twenty-first Annual International Pittsburgh Coal Conference "Coal - Energy and the Environment," CD-ROM Proceedings, paper no. 47-5 (pdf file #30), 17 pp., PCC, 2004, ISBN 1-890977-21-7. Pittsburgh Coal Conference (PCC), 1249 Benedum Hall, University of Pittsburgh, Pittsburgh, PA, 15261, USA, United States, p. Medium: ED.

Gerdemann, S.J., O'Connor, W.K., Dahlin, D.C., Penner, L.R., Rush, H., 2007a. Ex situ aqueous mineral carbonation. Environ. Sci. Technol. 41 (7), 2587–2593. doi:10.1021/es0619253.

Gerdemann, S.J., O'Connor, W.K., Dahlin, D.C., Penner, L.R., Rush, H., 2007b. *Ex Situ* aqueous mineral carbonation. Environ. Sci. Technol. 41 (7), 2587–2593. doi:10.1021/es0619253.

Giammar, D.E., Bruant, R.G., Peters, C.A., 2005. Forsterite dissolution and magnesite precipitation at conditions relevant for deep saline aquifer storage and sequestration of carbon dioxide. Chem. Geol. 217, 257–276.

Gielen, D., 2003. Uncertainties in relation to CO 2 capture and sequestration. Preliminary results.

Gíslason, S.R., Sigurdardóttir, H., Aradóttir, E.S., Oelkers, E.H., 2018. A brief history of CarbFix: challenges and victories of the project's pilot phase. Energy Procedia 146, 103–114.

Gualtieri, A.F., Giacobbe, C., Viti, C., 2012. The dehydroxylation of serpentine group minerals. Am. Mineral. 97, 666–680.

Gupta, N., Ball, D., Jagucki, P., Bradbury, J., 2009. Validating geologic storage potential in the midwestern USA through multiple field demonstrations. Energy Procedia 1 (1), 2063–2069. doi:10.1016/j.egypro.2009.01.269.

Gutknecht, V., Snæbjörnsdóttir, S.Ó., Sigfússon, B., Aradóttir, E.S., Charles, L., 2018. Creating a carbon dioxide removal solution by combining rapid mineralization of CO2 with direct air capture. Energy Procedia 146, 129–134. doi:10.1016/j.egypro.2018.07.017.

Hafner, M., Raimondi, P.P., Bonometti, B., 2023. Low-carbon energy strategies in MENA countries In: Hafner, M., Raimondi, P.P., Bonometti, B. (Eds.), The Energy Sector and Energy Geopolitics in the MENA Region at a Crossroad: Towards a Great Transformation? Springer International Publishing, Cham, pp. 175–261. doi:10.1007/978-3-031-30705-8_4.

Haug, T.A., Kleiv, R.A., Munz, I.A., 2010. Investigating dissolution of mechanically activated olivine for carbonation purposes. Appl. Geochem. 25 (10), 1547–1563. doi:10.1016/j.apgeochem.2010.08.005.

Hills, C.D., Tripathi, N., Carey, P.J., 2020. Mineralization technology for carbon capture, utilization, and storage. Front. Energy Res. 8. doi:10.3389/fenrg.2020.00142.

Hu, L., Bayer, P., Brauchler, R., 2016. Detection of carbon dioxide leakage during injection in deep saline formations by pressure tomography. Water. Resour. Res. 52 (7), 5676–5686. doi:10.1002/2015WR018420.

Huijgen, W., Comans, R., Witkamp, G.J., 2007a. Cost evaluation of CO2 sequestration by aqueous mineral carbonation. Energy Convers. Manage 48, 1923–1935. doi:10.1016/j.enconman.2007.01.035.

Huijgen, W.J.J., Comans, R.N.J., 2006. Carbonation of steel slag for CO2 sequestration: leaching of products and reaction mechanisms. Environ. Sci. Technol. 40 (8), 2790–2796. doi:10.1021/es052534b.

Huijgen, W.J.J., Comans, R.N.J., Witkamp, G.J., 2007b. Cost evaluation of CO2 sequestration by aqueous mineral carbonation. Energy Convers. Manage 48 (7), 1923–1935. doi:10.1016/j.enconman.2007.01.035.

Huijgen, W.J.J., Ruijg, G.J., Comans, R.N.J., Witkamp, G.J., 2006a. Energy consumption and net CO2 sequestration of aqueous mineral carbonation. Ind. Eng. Chem. Res. 45 (26), 9184–9194. doi:10.1021/ie060636k.

Huijgen, W.J.J., Witkamp, G.J., Comans, R.N.J., 2006b. Mechanisms of aqueous wollastonite carbonation as a possible CO2 sequestration process. Chem. Eng. Sci. 61 (13), 4242–4251. doi:10.1016/j.ces.2006.01.048.

Huijgen, W.J.J., Witkamp, G.J., Comans, R.N.J., 2006. Mechanisms of aqueous wollastonite carbonation as a possible CO2 sequestration process. Chem. Eng. Sci. 61, 4242–4251.

Hunt, A.J., Sin, E.H.K., Marriott, R., Clark, J.H., 2010. Generation, capture, and utilization of industrial carbon dioxide. ChemSusChem. 3 (3), 306–322. doi:10.1002/cssc.200900169.

Huo, D., Jalali, Y., 2010. An analysis of CO2 storage prospects in deep saline reservoirs. SPE Production and Operations Conference and Exhibition.

Ian Havercroft, N.R., 2023. CCS Legal and Regulatory Indicator 2023

IEA, I.E.A., 2023. Legal and regulatory frameworks for CCUS An IEA CCUS handbook.

IEF, I.E.F., 2024a. CCUS Regulatory and policy landscape a global and MENA perspective.

IEF, I.E.F., 2024b. Market assessment for CCUS in MENA region.

Jamil, M., Ahmad, F., Jeon, Y.J., 2016. Renewable energy technologies adopted by the UAE: prospects and challenges – A comprehensive overview. Renew. Sustain. Energy Rev. 55, 1181–1194. doi:10.1016/j.rser.2015.05.087.

Kelemen, P., Benson, S.M., Pilorgé, H., Psarras, P., Wilcox, J., 2019. An Overview of the status and challenges of CO2 storage in minerals and geological formations. Front. Clim. 1. doi:10.3389/fclim.2019.00009.

Kelemen, P.B., McQueen, N., Wilcox, J., Renforth, P., Dipple, G., Vankeuren, A.N.P., 2020. Engineered carbon mineralization in ultramafic rocks for CO2 removal from air: review and new insights. Chem. Geol. 550, 119628.

Khoo, H.H., Bu, J., Wong, R.L., Kuan, S.Y., Sharratt, P.N., 2011. Carbon capture and utilization: preliminary life cycle CO2, energy, and cost results of potential mineral carbonation. Energy Procedia 4, 2494–2501. doi:10.1016/j.egypro.2011.02.145.

Khoo, H.H., Tan, R.B.H., 2006. Life cycle evaluation of CO2 recovery and mineral sequestration alternatives. Environ. Progress 25 (3), 208–217. doi:10.1002/ep.10139.

Khoo, Z.Y., Ho, E.H.Z., Li, Y., Yeo, Z., Low, J.S.C., Bu, J., Chia, L.S.O., 2021. Life cycle assessment of a CO2 mineralisation technology for carbon capture and utilisation in Singapore. J. CO2 Util. 44, 101378. doi:10.1016/j.jcou.2020.101378.

Kongsjorden, H., Kårstad, O., Torp, T.A., 1998. Saline aquifer storage of carbon dioxide in the Sleipner project. Waste Manage. 17 (5), 303–308. doi:10.1016/S0956-053X(97)10037-X.

Koytsoumpa, E.I., Bergins, C., Kakaras, E., 2018. The CO2 economy: review of CO2 capture and reuse technologies. J. Supercrit. Fluids. 132, 3–16. doi:10.1016/j.supflu.2017.07.029.

Kusin, F.M., Hasan, S.N.M.S., Molahid, V.L.M., Yusuff, F.M., Jusop, S., 2023. Carbon dioxide sequestration of iron ore mining waste under low-reaction condition of a direct mineral carbonation process. Environ. Sci. Pollut. Res. 30 (9), 22188–22210. doi:10.1007/s11356-022-23677-3.

Kwak, J.H., Hu, J.Z., Turcu, R.V.F., Rosso, K.M., Ilton, E.S., Wang, C., Sears, J.A., Engelhard, M.H., Felmy, A.R., Hoyt, D.W., 2011. The role of H2O in the carbonation of forsterite in supercritical CO2. Int. J. Greenhouse Gas Control 5 (4), 1081–1092. doi:10.1016/j.ijggc.2011.05.013.

Lahn, B., 2021. Changing climate change: the carbon budget and the modifying-work of the IPCC. Soc. Stud. Sci. 51 (1), 3–27. doi:10.1177/0306312720941933.

Li, J., Hitch, M., 2017. Ultra-fine grinding and mechanical activation of mine waste rock using a planetary mill for mineral carbonation. Int. J. Miner. Process. 158, 18–26. doi:10.1016/j.minpro.2016.11.016.

Li, J., Hitch, M., 2018. Economic analysis on the application of mechanical activation in an integrated mineral carbonation process. Int. Biodeterior. Biodegradation 128, 63–71. doi:10.1016/j.ibiod.2016.08.026.

Li, J., Jacobs, A.D., Hitch, M., 2022. The effect of mineral composition on direct aqueous carbonation of ultramafic mine waste rock for CO2 sequestration, a case study of Turnagain ultramafic complex in British Columbia, Canada. Int. J. Min. Reclam. Environ. 36 (4), 267–286. doi:10.1080/17480930.2022.2041340.

Lindeberg, E., Vuillaume, J.F., Ghaderi, A., 2009. Determination of the CO2 storage capacity of the Utsira formation. Energy Procedia 1 (1), 2777–2784. doi:10.1016/j.egypro.2009.02.049.

Machado e Silva, I.M., Costa, H.K.M., 2021. Chapter 7 - the United Kingdom's experience in carbon capture and storage projects: the current regulatory framework and related challenges. In: de Medeiros Costa, H.K., Arlota, C. (Eds.), Carbon Capture and Storage in International Energy Policy and Law. Elsevier, pp. 141–153. doi:10.1016/B978-0-323-85250-0.00001-3.

Maina, J.W., Pringle, J.M., Razal, J.M., Nunes, S., Vega, L., Gallucci, F., Dumée, L.F., 2021. Strategies for integrated capture and conversion of CO2 from dilute flue gases and the atmosphere. ChemSusChem. 14 (8), 1805–1820. doi:10.1002/cssc.202100010.

Maroto-Valer, M.M., Tang, Z., Zhang, Y., 2005a. CO2 capture by activated and impregnated anthracites. Fuel Process. Technol. 86 (14), 1487–1502. doi:10.1016/j.fuproc.2005.01.003.

Maroto-Valer, M.M., Tang, Z., Zhang, Y., 2005b. CO2 capture by activated and impregnated anthracites. Fuel Process. Technol. 86, 1487–1502.

Marshall, J.P., 2022. A Social exploration of the west Australian gorgon gas, carbon capture and storage project. Clean Technol. 4 (1), 67–90.

McAdam, A.C., Zolotov, M.Y., Sharp, T.G., Leshin, L.A., 2008. Preferential low-pH dissolution of pyroxene in plagioclase–pyroxene mixtures: implications for martian surface materials. Icarus 196 (1), 90–96. doi:10.1016/j.icarus.2008.01.008.

McGrail, B.P., Schaef, H.T., Spane, F.A., Horner, J.A., Owen, A.T., Cliff, J.B., Qafoku, O., Thompson, C.J., Sullivan, E.C., 2017. Wallula basalt pilot demonstration project: post-injection results and conclusions. Energy Procedia 114, 5783–5790. doi:10.1016/j.egypro.2017.03.1716.

McGrail, B.P., Spane, F.A., Amonette, J.E., Thompson, C.R., Brown, C.F., 2014. Injection and monitoring at the wallula basalt pilot project. Energy Procedia 63, 2939–2948. doi:10.1016/j.egypro.2014.11.316.

Milne, P., 2021. Gorgon Emissions to Soar until Chevron Fixes Restricted CO2 Injection. BoilingCold.

Moghadam, H.S., Stern, R.J., 2015. Ophiolites of Iran: keys to understanding the tectonic evolution of SW Asia: (II) Mesozoic ophiolites. J. Asian Earth. Sci. 100, 31–59. doi:10.1016/j.jseaes.2014.12.016.

Molahid, V.L.M., Mohd Kusin, F., Syed Hasan, S.N.M., Ramli, N.A.A., Abdullah, A.M., 2022. CO2 Sequestration through mineral carbonation: effect of different parameters on carbonation of Fe-Rich mine waste materials. Processes 10 (2), 432.

Mora Mendoza, E.Y., Sarmiento Santos, A., Vera López, E., Drozd, V., Durygin, A., Chen, J., Saxena, S.K., 2019. Iron oxides as efficient sorbents for CO2 capture. J. Mater. Res. Technol. 8 (3), 2944–2956. doi:10.1016/j.jmrt.2019.05.002.

Moucha, R., Forte, A.M., 2011. Changes in African topography driven by mantle convection. Nat. Geosci. 4 (10), 707–712. doi:10.1038/ngeo1235.

Moufti, M.R., Moghazi, A.M., Ali, K.A., 2012. Geochemistry and Sr–Nd–Pb isotopic composition of the harrat al-madinah volcanic field, Saudi Arabia. Gondwana Res. 21 (2), 670–689. doi:10.1016/j.gr.2011.06.003.

Moufti, M.R., Moghazi, A.M., Ali, K.A., 2013. 40Ar/39Ar geochronology of the Neogene-Quaternary Harrat Al-Madinah intercontinental volcanic field, Saudi Arabia: implications for duration and migration of volcanic activity. J. Asian Earth. Sci. 62, 253–268. doi:10.1016/j.jseaes.2012.09.027.

Munz, I.A., Brandvoll, Ø., Haug, T.A., Iden, K., Smeets, R., Kihle, J., Johansen, H., 2012. Mechanisms and rates of plagioclase carbonation reactions. Geochim. Cosmochim. Acta 77, 27–51. doi:10.1016/j.gca.2011.10.036.

Naraharisetti, P.K., Yeo, T.Y., Bu, J., 2019. New classification of CO2 mineralization processes and economic evaluation. Renew. Sustain. Energy Rev. 99, 220–233. doi:10.1016/j.rser.2018.10.008.

National Academies of Sciences, E., Medicine, 2019. Negative Emissions Technologies and Reliable Sequestration: A Research Agenda. The National Academies Press, Washington, DC doi:10.17226/25259.

Nduagu, E., Bergerson, J., Zevenhoven, R., 2012. Life cycle assessment of CO2 sequestration in magnesium silicate rock – A comparative study. Energy Convers. Manage 55, 116–126. doi:10.1016/j.enconman.2011.10.026.

Necibi, M.C., Brouziyne, Y., Chehbouni, A., 2022. Chapter 14 - Decarbonization: regulation and policies. In: Khalid, M., Dharaskar, S.A., Sillanpää, M., Siddiqui, H. (Eds.), Emerging Carbon Capture Technologies. Elsevier, pp. 401–426. doi:10.1016/B978-0-323-89782-2.00009-0.

Neeraj, Yadav, S., 2020. Carbon storage by mineral carbonation and industrial applications of CO2. Mater. Sci. Energy Technol. 3, 494–500. doi:10.1016/j.mset.2020.03.005.

O'Connor, W., Dahlin, D., Rush, G., Gerdemann, S., Penner, L., Nilsen, D., 2005. Aqueous Mineral Carbonation. DOE, US.

O'Connor, W.K., Dahlin, D.C., Rush, G.E., Dahlin, C.L., Collins, W.K., 2002. Carbon dioxide sequestration by direct mineral carbonation: process mineralogy of feed and products. Mining. Metall. Exploration 19 (2), 95–101. doi:10.1007/BF03403262.

Oconnor, W., Dahlin, D.C., Rush, G.E., Gerdemann, S.J., Penner, L.R., Nilsen, D.N., 2005. Aqueous mineral carbonation: mineral availability, pretreatment, reaction parametrics, and process studies. https://doi.org/10.13140/RG.2.2.23658.31684.

Olajire, A.A., 2013. A review of mineral carbonation technology in sequestration of CO2. J. Petrol. Sci. Eng. 109, 364–392. doi:10.1016/j.petrol.2013.03.013.

Ostovari, H., Sternberg, A., Bardow, A., 2020. Rock 'n' use of CO2: carbon footprint of carbon capture and utilization by mineralization. Sustain. Energy Fuels. 4 (9), 4482–4496. doi:10.1039/D0SE00190B.

Park, A.H.A., Fan, L.S., 2004. CO2 mineral sequestration: physically activated dissolution of serpentine and pH swing process. Chem. Eng. Sci. 59 (22), 5241–5247. doi:10.1016/j.ces.2004.09.008.

Park, A.H.A., Jadhav, R., Fan, L.S., 2003. CO2 mineral sequestration: chemically enhanced aqueous carbonation of serpentine. Can. J. Chem. Eng. 81 (3–4), 885–890. doi:10.1002/cjce.5450810373.

Pasquier, L.C., Mercier, G., Blais, J.F., Cecchi, E., Kentish, S., 2016. Technical & economic evaluation of a mineral carbonation process using southern Québec mining wastes for CO2 sequestration of raw flue gas with by-product recovery. Int. J. Greenhouse Gas Control 50, 147–157. doi:10.1016/j.ijggc.2016.04.030.

Paul, S., Bera, S., Dasgupta, R., Mondal, S., Roy, S., 2021. Review on the recent structural advances in open and closed systems for carbon capture through algae. Energy Nexus. 4, 100032. doi:10.1016/j.nexus.2021.100032.

Peltonen, P., 2005. Chapter 6 Ophiolites. In: Lehtinen, M., Nurmi, P.A., Rämö, O.T. (Eds.), Developments in Precambrian Geology. Elsevier, pp. 237–277. doi:10.1016/S0166-2635(05)80007-6.

Penner, L.R., O'Connor, W.K., Dahlin, D.C., Gerdemann, S.J., Rush, G.E., 2004a. Mineral carbonation: Energy Costs of Pretreatment Options and Insights Gained from Flow Loop Reaction Studies. Albany Research Center (ARC), Albany, OR (United States).

Penner, L.R., O'Connor, W.K., Dahlin, D.C., Gerdemann, S.J., Rush, G.E., 2004b. Mineral carbonation: energy costs of pretreatment options and insights gained from flow loop reaction studies. In: Conference: 3rd Annual Conference on Carbon Capture & Sequestration. Alexandria, VA May 3-6, 2004 (sponsored by the National Energy Technology Laboratory, US Dept. of Energy); Related Information: Presented as a poster session with full text published on CD of Proceedings. Exchange Monitor Publications & Forums, Washington, DC, United States, p. Medium: ED.

Power, I.M., Harrison, A.L., Dipple, G.M., Wilson, S., Kelemen, P.B., Hitch, M., Southam, G., 2013. Carbon mineralization: from natural analogues to engineered systems. Rev. Mineral. Geochem. 77 (1), 305–360. doi:10.2138/rmg.2013.77.9.

Ragnheidardottir, E., Sigurdardottir, H., Kristjansdottir, H., Harvey, W., 2011. Opportunities and challenges for CarbFix: an evaluation of capacities and costs for the pilot scale mineralization sequestration project at Hellisheidi, Iceland and beyond. Int. J. Greenhouse Gas Control 5 (4), 1065–1072. doi:10.1016/j.ijggc.2010.11.010.

Rashid, M.I., Yaqoob, Z., Mujtaba, M.A., Fayaz, H., Saleel, C.A., 2023. Developments in mineral carbonation for Carbon sequestration. Heliyon. e21796. doi:10.1016/j.heliyon.2023.e21796.

Rasool, M.H., Ahmad, M., 2023. Reactivity of basaltic minerals for CO2 sequestration via in situ mineralization: a review. Minerals 13 (9), 1154.

Raza, A., Glatz, G., Gholami, R., Mahmoud, M., Alafnan, S., 2022. Carbon mineralization and geological storage of CO2 in basalt: mechanisms and technical challenges. Earth. Sci. Rev. 229, 104036. doi:10.1016/j.earscirev.2022.104036.

Rigopoulos, I., Harrison, A.L., Delimitis, A., Ioannou, I., Efstathiou, A.M., Kyratsi, T., Oelkers, E.H., 2018. Carbon sequestration via enhanced weathering of peridotites and basalts in seawater. Appl. Geochem. 91, 197–207. doi:10.1016/j.apgeochem.2017.11.001.

Romano, M.C., Anantharaman, R., Arasto, A., Ozcan, D.C., Ahn, H., Dijkstra, J.W., Carbo, M., Boavida, D., 2013. Application of advanced technologies for CO2 capture from industrial sources. Energy Procedia 37, 7176–7185. doi:10.1016/j.egypro.2013.06.655.

Romanov, V., Soong, Y., Carney, C., Rush, G.E., Nielsen, B., O'Connor, W., 2015. Mineralization of carbon dioxide: a literature review. ChemBioEng Rev. 2 (4), 231–256. doi:10.1002/cben.201500002.

Romão, I.S., Gando-Ferreira, L.M., da Silva, M.M.V.G., Zevenhoven, R., 2016. CO2 sequestration with serpentinite and metaperidotite from Northeast Portugal. Miner. Eng. 94, 104–114. doi:10.1016/j.mineng.2016.05.009.

Sanna, A., Uibu, M., Caramanna, G., Kuusik, R., Maroto-Valer, M.M., 2014. A review of mineral carbonation technologies to sequester CO2. Chem. Soc. Rev. 43 (23), 8049–8080. doi:10.1039/C4CS00035H.

Schott, J., Berner, R.A., Sjöberg, E.L., 1981. Mechanism of pyroxene and amphibole weathering—I. Experimental studies of iron-free minerals. Geochim. Cosmochim. Acta 45 (11), 2123–2135. doi:10.1016/0016-7037(81)90065-X.

Searle, M., Rioux, M., Garber, J.M., 2022. One line on the map: a review of the geological history of the Semail Thrust, Oman-UAE mountains. J. Struct. Geol. 158, 104594. doi:10.1016/j.jsg.2022.104594.

Searle, M.P., Ali, M.Y., 2009. Structural and tectonic evolution of the Jabal Sumeini-Al Ain-Buraimi region, northern Oman and eastern United Arab Emirates. GeoArabia 14 (1), 115–142.

Searle, M.P., Cox, J.O.N., 2002. Subduction zone metamorphism during formation and emplacement of the Semail ophiolite in the Oman Mountains. Geol. Mag. 139 (3), 241–255. doi:10.1017/S0016756802006532.

Searle, M.P., Waters, D.J., Garber, J.M., Rioux, M., Cherry, A.G., Ambrose, T.K., 2015. Structure and metamorphism beneath the obducting Oman ophiolite: evidence from the Bani Hamid granulites, northern Oman mountains. Geosphere 11 (6), 1812–1836. doi:10.1130/ges01199.1.

Shah, S., Shah, M., Shah, A., Shah, M., 2020. Evolution in the membrane-based materials and comprehensive review on carbon capture and storage in industries. Emergent. Mater. 3 (1), 33–44. doi:10.1007/s42247-020-00069-2.

Shukla, R., Ranjith, P., Haque, A., Choi, X., 2010. A review of studies on CO2 sequestration and caprock integrity. Fuel 89 (10), 2651–2664. doi:10.1016/j.fuel.2010.05.012.

Snæbjörnsdóttir, S.Ó., Sigfússon, B., Marieni, C., Goldberg, D., Gislason, S.R., Oelkers, E.H., 2020. Carbon dioxide storage through mineral carbonation. Nature Rev.Earth Environ. 1 (2), 90–102. doi:10.1038/s43017-019-0011-8.

Stasiulaitiene, I., Vajegaite, V., Martuzevicius, D., Denafas, G., Sliaupa, S., Fagerlund, J., Zevenhoven, R., 2014. Parameters affecting Mg(OH)2 extraction from serpentinites in lithuania for the purpose of CO2 reduction by mineral carbonation. Environ. Prog. Sustain. Energy 33 (2), 512–518. doi:10.1002/ep.11792.

Summers, C.A., Dahlin, D.C., Rush, G.E., O'Connor, W.K., Gerdemann, S.J., 2005. Grinding methods to enhance the reactivity of olivine. Mining. Metall. Exploration 22 (3), 140–144. doi:10.1007/BF03403128.

Teir, S., Kuusik, R., Fogelholm, C.J., Zevenhoven, R., 2007a. Production of magnesium carbonates from serpentinite for long-term storage of CO2. Int. J. Miner. Process. 85, 1–15.

Teir, S., Kuusik, R., Fogelholm, C.J., Zevenhoven, R., 2007b. Production of magnesium carbonates from serpentinite for long-term storage of CO2. Int. J. Miner. Process. 85 (1), 1–15. doi:10.1016/j.minpro.2007.08.007.

Tiefenthaler, J., Braune, L., Bauer, C., Sacchi, R., Mazzotti, M., 2021. Technological demonstration and life cycle assessment of a negative emission value chain in the swiss concrete sector. Front. Clim. 3. doi:10.3389/fclim.2021.729259.

Torp, T.A., Brown, K.R., et al., 2005. - CO2 underground storage costs as experienced at Sleipner and Weyburn. In: Rubin, E.S., Keith, D.W., Gilboy, C.F., Wilson, M., Morris, T., Gale, J., et al. (Eds.), Greenhouse Gas Control Technologies 7. Elsevier Science Ltd, Oxford, pp. 531–538. doi:10.1016/B978-008044704-9/50054-9.

Torp, T.A., Gale, J., 2004. Demonstrating storage of CO2 in geological reservoirs: the Sleipner and SACS projects. Energy 29 (9), 1361–1369. doi:10.1016/j.energy.2004.03.104.

Truong, T.H., Lin, B.W., Lo, C.H., Tung, C.P., Chao, C.W., 2024. Possible pathways for low carbon transitions: investigating the efforts of oil companies in CCUS technologies. Energy Strategy Rev. 54, 101421. doi:10.1016/j.esr.2024.101421.

TuysuzNecati, ErlerAyhan, 1993. Geochemistry and evolution of listwaenites in the Kagizman region (Kars, NE-Turkey). Chemie der Erde 53 (4), 315–329.

Urey, H.C., Korff, S.A., 1952. The planets: their origin and development. Phys Today 5 (8). doi:10.1063/1.3067687, 12-12.

Vahrenkamp, V., Afif, A., Tasianas, A., Hoteit, H., 2021. The geological potential of the arabian plate for CCS and CCUS-an overview. In: Proceedings of the 15th Greenhouse Gas Control Technologies Conference, pp. 15–18.

Vikram Vishal, P.P., Ingvild Ombudstvedt, George Koperna, 2024. Carbon capture, utilization and storage: handbook for policymakers.

Wakabayashi, M., Kimura, O., 2018. The impact of the Tokyo metropolitan emissions trading scheme on reducing greenhouse gas emissions: findings from a facility-based study. Clim. Policy. 18 (8), 1028–1043. doi:10.1080/14693062.2018.1437018.

Wang, B., Pan, Z., Cheng, H., Zhang, Z., Cheng, F., 2021. A review of carbon dioxide sequestration by mineral carbonation of industrial byproduct gypsum. J. Clean. Prod. 302, 126930. doi:10.1016/j.jclepro.2021.126930.

Wang, F., Dreisinger, D., Jarvis, M., Hitchins, T., 2019. Kinetics and mechanism of mineral carbonation of olivine for CO2 sequestration. Miner. Eng. 131, 185–197. doi:10.1016/j.mineng.2018.11.024.

Wang, X., Maroto-Valer, M.M., 2011. Integration of CO2 capture and mineral carbonation by using recyclable ammonium salts. ChemSusChem. 4 (9), 1291–1300. doi:10.1002/cssc.201000441.

Woodall, C.M., McQueen, N., Pilorgé, H., Wilcox, J., 2019. Utilization of mineral carbonation products: current state and potential. Greenhouse Gases: Sci. Technol. 9 (6), 1096–1113. doi:10.1002/ghg.1940.

Yafiee, O.A., Mumtaz, F., Kumari, P., Karanikolos, G.N., Decarlis, A., Dumée, L.F., 2024. Direct air capture (DAC) vs. Direct ocean capture (DOC)–A perspective on scale-up demonstrations and environmental relevance to sustain decarbonization. Chem. Eng. J. 497, 154421. doi:10.1016/j.cej.2024.154421.

Zhang, J., Zhang, R., Geerlings, H., Bi, J., 2012. Mg-silicate carbonation based on an HCl- and NH3-recyclable process: effect of carbonation temperature. Chem. Eng. Technol. 35 (3), 525–531. doi:10.1002/ceat.201100425.

Zhao, L., Sang, L., Chen, J., Ji, J., Teng, H.H., 2010. Aqueous carbonation of natural brucite: relevance to CO2 sequestration. Environ. Sci. Technol. 44 (1), 406–411. doi:10.1021/es9017656.

Zhou, D.D., Zhang, X.W., Mo, Z.W., Xu, Y.Z., Tian, X.Y., Li, Y., Chen, X.M., Zhang, J.P., 2019. Adsorptive separation of carbon dioxide: from conventional porous materials to metal–organic frameworks. EnergyChem 1 (3), 100016. doi:10.1016/j.enchem.2019.100016.